SIAM Review
Vol. 62, No. 4, pp. 901–935

© 2020 Society for Industrial and Applied Mathematics

Downloaded 10/30/20 to 59.64.129.2. Redistribution subject to SIAM license or copyright; see https://epubs.siam.org/page/terms

Time Correlation Functions of Equilibrium and Nonequilibrium Langevin Dynamics: Derivations and Numerics Using Random Numbers*

Xiaocheng Shang†
Martin Kröger‡

Abstract. We study the time correlation functions of coupled linear Langevin dynamics with and without inertial effects, both analytically and numerically. The model equation represents the physical behavior of a harmonic oscillator in two or three dimensions in the presence of friction, additive noise, and an external field with both rotational and deformational components. This simple model plays pivotal roles in understanding more complicated processes. The analytical solution presented serves as a test of numerical integration schemes, and its derivation is presented in a fashion that allows it to be repeated directly in a classroom. While the results in the absence of fields (equilibrium) or confinement (free particle) are omnipresent in the literature, we write down, apparently for the first time, the full nonequilibrium results that may correspond, e.g., to a Hookean dumbbell embedded in a macroscopically homogeneous shear or mixed flow field. We demonstrate how the inertial results reduce to their noninertial counterparts in the nontrivial limit of vanishing mass. While the results are derived using basic integrations over Dirac delta distributions, we also provide alternative approaches involving (i) Fourier transforms, which seem advantageous only if the measured quantities also reside in Fourier space, and (ii) a Fokker–Planck equation and the moments of the probability distribution. The results, verified by numerical experiments, provide additional means of measuring the performance of numerical methods for such systems. It should be emphasized that this article provides specific details regarding the derivations of the time correlation functions as well as the implementations of various numerical methods, so that it can serve as a standalone piece for lessons in the framework of Itô stochastic differential equations and calculus.

Key words. time correlation functions, stochastic differential equations, Brownian/Langevin dynamics, harmonic oscillator, nonequilibrium, numerical integration

AMS subject classifications. 65C30, 60H35, 37M25

DOI. 10.1137/19M1255471

Contents

*Received by the editors April 10, 2019; accepted for publication (in revised form) October 28, 2019; published electronically November 3, 2020.
https://doi.org/10.1137/19M1255471

†Department of Materials, Polymer Physics, ETH Zurich, Leopold-Ruzicka-Weg 4, CH-8093 Zurich, Switzerland. Current address: School of Mathematics, University of Birmingham, Birmingham, B15 2TT, United Kingdom (x.shang.1@bham.ac.uk).
‡Department of Materials, Polymer Physics, ETH Zurich, Leopold-Ruzicka-Weg 4, CH-8093 Zurich, Switzerland (mk@mat.ethz.ch, http://www.complexfluids.ethz.ch).

Copyright © by SIAM. Unauthorized reproduction of this article is prohibited.

1. Introduction. The efficiency and accuracy of numerical solvers for Itô stochastic differential equations (SDEs), including those that are equivalent to diffusion-type partial differential equations, are difficult to assess without access to analytical reference solutions. Only for the simplest linear cases can transient moments and time

Downloaded 10/30/20 to 59.64.129.2. Redistribution subject to SIAM license or copyright; see https://epubs.siam.org/page/terms

Copyright © by SIAM. Unauthorized reproduction of this article is prohibited.

Downloaded 10/30/20 to 59.64.129.2. Redistribution subject to SIAM license or copyright; see https://epubs.siam.org/page/terms

correlation functions be calculated analytically. For nonlinear SDEs, analytical solutions are generally not available; nevertheless, convergence and stability issues have been discussed [9, 23, 55]. Here we propose an essentially two-dimensional nontrivial, still linear benchmark problem (see the Langevin dynamics problem (2.13)), inspired by the challenging problem of the dynamics of macromolecules, which is still exactly solvable. It includes inertial effects, which are usually neglected as they pose extra problems and because their physical significance is a priori unclear, or because any possible related effects are considered "small."

The benchmark equation we are going to consider arises in several different contexts, where linear restoring forces compete with stochastic additive noise, in the presence of an external field, while the absence of either the restoring force or the external field are both popular special cases that include, for example, the random walk [10, 50], diffusion [19, 25, 62], a charged atom in an electric field [27], the motion of atoms in the presence of gravitational, centrifugal, chemical potential, etc., gradients [45], RNA unfolding via laser tweezers [46], nanomagnets subjected to magnetic fields and superparamegnetization [11], Brownian oscillators [11], dielectric and magnetic permittivity in dilute solutions of macromolecules [8] or ferrofluids [16], phoretic forces [31], vibration and photodesorption of diatomic gases [44], and rotational relaxation of molecules trapped in a three-dimensional crystal [13]. Including inertial effects in Brownian dynamics (i.e., the overdamped limit of the Langevin dynamics), where they are usually neglected, can help understand the origins of departures from the expected behavior, especially at short times, for tracer nanoparticles experiencing both inertial and stochastic forces, in microrheology, or to explain the occurrence of negative storage moduli [4, 5, 49, 67].

Let us introduce one explicit example from the world of polymer physics, dealing with macromolecules, DNA, and actin filaments and the like, as well as materials, biochemical, and engineering sciences, which is captured by our benchmark problem. The dynamics of a single flexible polymer dissolved in Newtonian solvent and flexible polymers confined in melts are both, to a first approximation, well captured by the Brownian motion of a linear chain consisting of a number of identical mass points (or beads), permanently interconnected by harmonic springs and interacting with the surroundings via Gaussian white noise [14, 53]. In that case the harmonic spring results are based upon the assumptions that each partial chain, thought to reside between and terminate at the mass points, behaves as an ideal chain that can be mapped using Kuhn's approach to a random walk. Assuming that Stokes' friction hinders the free motion of the mass points due to frequent collisions with the surrounding medium, the strength of the additive noise is related to the bead friction coefficient via a fluctuation-dissipation relation. The rheological, viscoelastic properties of polymers are very different from those of simple liquids, and can be studied by considering a polymer dissolved in a solution that is not at rest, but subjected to a flow gradient. While the precise trajectory of the polymer is unavailable because of the stochastic noise, measurable time correlation functions can be calculated analytically in the weak sense (see more discussions in subsection 4.1). Since polymeric systems are often overdamped, the inertia, which is quantified by the mass, is thus typically neglected, and this is known as the Rouse model [7, 56] (i.e., in the form of the Brownian dynamics). However, as pointed out in [57], the inertia of the chains might be expected to be more important for samples in solvents of extremely low viscosity, e.g., "supercritical solvents," due to the fact that the dimensionless mass depends inversely upon the solvent viscosity squared. Upon introducing normal coordinates [14, 15], the differ-

Copyright © by SIAM. Unauthorized reproduction of this article is prohibited.

Downloaded 10/30/20 to 59.64.129.2. Redistribution subject to SIAM license or copyright; see https://epubs.siam.org/page/terms

ential equations that need to be solved to treat the complete polymer problem with masses [29], and for polymers subjected to a macroscopic homogeneous flow field [32], are identical to the equations of motion of a harmonic oscillator with a single mass, connected with the origin by a spring.

Inertial effects in the context of microbead rheology [26], where the spring coefficient k is due to an optical trap, appear to improve the agreement with data for dynamical viscosities at high frequencies [66]. The inertial effects are known to be quite irrelevant under most common conditions, but should increase with the increasing size of the microbead and softness of the surrounding material [63]. It has also been demonstrated in [24] that including the inertial effects for the study of fluid suspensions is necessary. Furthermore, in the context of molecular dynamics, the inclusion of the inertial effects leads to the possibilities of designing various thermostats, which are powerful tools for sampling the invariant measure [3, 18, 36].

This article is organized as follows. We present the model Langevin dynamics and its noninertial special (Brownian) case, and introduce dimensionless quantities in section 2 to come up with a dimensionless Langevin dynamics suitable for benchmark tests. In section 3, we derive the stationary time correlation functions of this equation both with and without inertial effects. In addition to demonstrating that the inertial results reduce to their noninertial counterparts in the limit of vanishing mass, we provide two alternative approaches based on (i) the Fourier transform and (ii) the Fokker–Planck equation to obtain the stationary time correlation functions. We review, in section 4, various numerical methods used to solve either Brownian dynamics or Langevin dynamics. The available correlation functions are important measures of dynamical fidelity that numerical integrators should be able to reproduce. Section 5 presents numerical experiments in both cases, not only verifying the analytical results but also comparing the performance of those numerical methods. A summary and outlook is given in section 6.

2. The Model Equation. Consider the linear Langevin dynamics with a single harmonic oscillator of mass m in the presence of a streaming background medium with velocity field $\mathbf{u}$, whose equations of motion for its extension, or end-to-end vector $\mathbf{q}(t)$, are given by[1]

$$m\ddot{\mathbf{q}} = -k\mathbf{q} - \gamma\,(\dot{\mathbf{q}} - \mathbf{u}) + \sigma\boldsymbol{\eta}(t)\,, \tag{2.1}$$

where a dot denotes a derivative with respect to time t, k represents a spring coefficient, and the positive friction coefficient γ and noise strength σ are related via a fluctuation-dissipation relation

$$\sigma^2 = 2\gamma k_{\mathrm{B}}T\,, \tag{2.2}$$

where k_{B} and T denote the Boltzmann constant and absolute temperature, respectively. The components of the time-dependent vector $\boldsymbol{\eta}(t)$ represent a "white noise" or "Brownian motion" term, usually modeled by the mutually independent increments of a continuous time-stochastic Wiener process [6]. The $\boldsymbol{\eta}(t)$ thus has a Gaussian probability distribution whose average and correlation function are given by

$$\langle\boldsymbol{\eta}(t)\rangle = \mathbf{0}\,, \qquad \langle\boldsymbol{\eta}(t)\,\boldsymbol{\eta}(t')\rangle = \mathbf{I}\,\delta(t-t')\,, \tag{2.3}$$

[1]Here we use the standard notation used in modern textbooks for physicists [14] or on Wikipedia, while the mathematics literature might prefer $\mathrm{d}\eta_t$ instead of $\eta(t)$.

Copyright © by SIAM. Unauthorized reproduction of this article is prohibited.

Downloaded 10/30/20 to 59.64.129.2. Redistribution subject to SIAM license or copyright; see https://epubs.siam.org/page/terms

where $\langle\cdot\rangle$ denotes an ensemble average and $\mathbf{I}$ is the unity matrix. The δ-distribution form of the correlations in time means that the force $\sigma\boldsymbol{\eta}(t)$ at a time t is assumed to be completely uncorrelated with it at any other time; $\boldsymbol{\eta}$ has units of $\mathrm{s}^{-1/2}$. For the purposes of this review, the properties (2.3) fully characterize the noise, and the additional requirement of a Gaussian probability is nowhere essential. When solving (2.1) we impose the initial conditions $\mathbf{q}(-\infty) = \lim_{t\to-\infty}\mathbf{q}(t) = \mathbf{0}$ and $\dot{\mathbf{q}}(-\infty) = \mathbf{0}$ as long as we are interested in stationary time correlation functions such as $\langle\mathbf{q}(t)\cdot\mathbf{q}(0)\rangle$ that are unaffected by the precise initial conditions and are thus symmetric in t in the absence of the assumed homogeneous streaming velocity field $\mathbf{u} = \boldsymbol{\kappa}\cdot\mathbf{q}$. The matrix $\boldsymbol{\kappa}$ (transposed macroscopic homogeneous velocity gradient) is arbitrary, and it is traceless for the case of incompressible flow. It can be generally decomposed into a symmetric and an antisymmetric part, representing the pure deformational and pure rotational parts of the flow field. If, furthermore, we choose a suitable coordinate system, the still arbitrary $\boldsymbol{\kappa}$ can be considered to have nonvanishing components only on its diagonal and on one of the nondiagonal components:

$$\boldsymbol{\kappa} = \begin{pmatrix} \kappa_{xx} & \kappa_{xy} & 0 \\ 0 & \kappa_{yy} & 0 \\ 0 & 0 & \kappa_{zz} \end{pmatrix}. \tag{2.4}$$

The rotational part of the flow field is thus solely specified by the so-called shear rate κ_{xy}, while the deformational component carries all components of $\boldsymbol{\kappa}$, i.e., the shear and three elongational rates. In the absence of $\mathbf{u}$ or for a diagonal (irrotational) $\boldsymbol{\kappa}$ tensor characterizing elongational flow, (2.1) is identical to three uncoupled equations for three scalar components, each of which describes a one-dimensional linear Langevin dynamics with inertia. In what follows we consider a more general case in which the system is subjected to a mixed flow with shear rate κ_{xy}. In this case, the equations of (2.1) for the components do not decouple anymore, and they instead read, with $\mathbf{q} = (x, y, z)$,

$$m\ddot{x} = -k_x x - \gamma\,(\dot{x} - \kappa_{xy} y) + \sigma\,\eta_x\,, \tag{2.5a}$$

$$m\ddot{y} = -k_y y - \gamma\dot{y} + \sigma\,\eta_y\,, \tag{2.5b}$$

and there is no need to write down an extra equation for the z-component, as it remains coupled to neither x- nor y-components. We have also introduced effective spring coefficients $k_\mu \equiv k - \gamma\kappa_{\mu\mu}, \mu \in \{x, y\}$, to incorporate potential contributions from the diagonal of the $\boldsymbol{\kappa}$ tensor. To improve the neatness of the presentation, we are going to introduce appropriate abbreviations below. It also turns out that it is useful to introduce different abbreviations for both the noninertial and the inertial cases.

For the noninertial ($m = 0$) case, associated with Brownian or overdamped Langevin dynamics, we can rewrite (2.5) as

$$\dot{x} = \kappa_{xy} y - \omega_x x + \sqrt{2D}\,\eta_x\,, \tag{2.6a}$$

$$\dot{y} = -\omega_y y + \sqrt{2D}\,\eta_y\,, \tag{2.6b}$$

having introduced (no summation convention unless otherwise stated) two characteristic frequencies ω_μ and a diffusion coefficient D:

$$\omega_\mu \equiv \frac{k_\mu}{\gamma} = \frac{k - \gamma\kappa_{\mu\mu}}{\gamma}, \qquad D \equiv \frac{\sigma^2}{2\gamma^2} = \frac{k_\mathrm{B}T}{\gamma}\,. \tag{2.7}$$

Copyright © by SIAM. Unauthorized reproduction of this article is prohibited.

Downloaded 10/30/20 to 59.64.129.2. Redistribution subject to SIAM license or copyright; see https://epubs.siam.org/page/terms

2.1. Connections with the Dumbbell Model. The so-called dumbbell model, where two masses m are connected by a spring with a spring coefficient k, is the simplest model to describe the behavior of a drastically coarse-grained polymer molecule, whose equations of motion (subject to shear with rate κ_{xy} and/or elongational flow whose rates are captured by anisotropic spring coefficients k_x and k_y) read

$$m\ddot{x}_1 = -k_x\,(x_1 - x_2) - \gamma\,(\dot{x}_1 - \kappa_{xy}y_1) + \sigma\eta_{x_1}\,, \tag{2.8a}$$

$$m\ddot{x}_2 = -k_x\,(x_2 - x_1) - \gamma\,(\dot{x}_2 - \kappa_{xy}y_2) + \sigma\eta_{x_2}\,, \tag{2.8b}$$

$$m\ddot{y}_1 = -k_y\,(y_1 - y_2) - \gamma\dot{y}_1 + \sigma\eta_{y_1}\,, \tag{2.8c}$$

$$m\ddot{y}_2 = -k_y\,(y_2 - y_1) - \gamma\dot{y}_2 + \sigma\eta_{y_2}\,. \tag{2.8d}$$

Introducing relative (end-to-end) vector components $X = x_2 - x_1$, $Y = y_2 - y_1$, center of mass coordinates $C_x = (x_1 + x_2)/2$, $C_y = (y_1 + y_2)/2$, and noting that $\sqrt{2}\,\eta_x = \eta_{x_1} \pm \eta_{x_2}$, (2.8) becomes

$$m\ddot{C}_x = -\gamma\left(\dot{C}_x - \kappa_{xy}C_y\right) + \frac{\sigma}{\sqrt{2}}\eta_x\,, \tag{2.9a}$$

$$m\ddot{C}_y = -\gamma\dot{C}_y + \frac{\sigma}{\sqrt{2}}\eta_y\,, \tag{2.9b}$$

$$m\ddot{X} = -2k_xX - \gamma\left(\dot{X} - \kappa_{xy}Y\right) + \sqrt{2}\sigma\eta_x\,, \tag{2.9c}$$

$$m\ddot{Y} = -2k_yY - \gamma\dot{Y} + \sqrt{2}\sigma\eta_y\,. \tag{2.9d}$$

These two uncoupled sets of equations for X, Y and C_x, C_y are of the form studied in subsections 3.3 and 3.4, respectively. With the new 1-variables $k_\mu^1 = 2k_\mu$, $\gamma_1 = \gamma$, and $\sigma_1^2 = 2\sigma^2 = 4\gamma k_{\mathrm{B}}T = 2\gamma_1 k_{\mathrm{B}}T_1$, the end-to-end vector of the elastic dumbbell behaves like a harmonic oscillator with mass m, unchanged friction coefficient γ, but modified spring coefficient $k_\mu^1 = 2k_\mu$ and temperature $T_1 = 2T$. Therefore, the stationary time correlation functions for the end-to-end vector $\mathbf{q}$ of the dumbbell model are identical to those obtained for the nonideal cases upon replacing T by $2T$ and k_μ by $2k_\mu$. Similarly, the dynamics of the center of mass of the dumbbell is captured by the results for the ideal (springless) cases upon replacing T by $T/2$. The overdamped (noninertial) cases of the dumbbell are thus also treated in subsections 3.1 and 3.2.

2.2. Nondimensionalization. In fact, we could have eliminated one more parameter by switching to dimensionless time. However, in order to prevent any confusion with the notation, we introduce dimensionless units only for the more advanced inertial case, where dimensionless units pay off more significantly. To this end we introduce dimensionless position and time for the inertial ($m > 0$) case via

$$x_* \equiv \frac{x}{q_{\mathrm{ref}}}\,, \qquad y_* \equiv \frac{y}{q_{\mathrm{ref}}}\,, \qquad t_* \equiv \frac{t}{t_{\mathrm{ref}}}\,, \tag{2.10}$$

where reference quantities q_{ref} and t_{ref} are chosen as

$$q_{\mathrm{ref}} \equiv \frac{\sigma\sqrt{m}}{(\gamma/2)^{3/2}} = \frac{4\sqrt{mk_{\mathrm{B}}T}}{\gamma}\,, \quad t_{\mathrm{ref}} \equiv \frac{2m}{\gamma}\,. \tag{2.11}$$

Upon further introducing dimensionless spring coefficients s_μ and a dimensionless shear rate r as

$$s_\mu \equiv \frac{4mk_\mu}{\gamma^2} = \frac{4m\omega_\mu}{\gamma}\,, \quad r \equiv \frac{2m\kappa_{xy}}{\gamma}\,, \tag{2.12}$$

Copyright © by SIAM. Unauthorized reproduction of this article is prohibited.

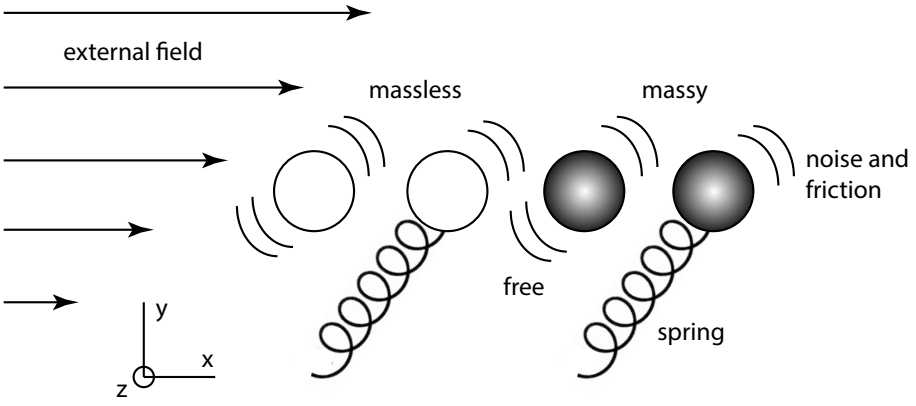

Fig. 1 *Schematic descriptions of a variety of possible conditions associated with the Langevin dynamics* (2.1) *in the presence of an external flow field (the shown arrows correspond to the case of pure shear). From left to right: free, massless, ideal Brownian; spring-connected, massless, nonideal Brownian; free, inertial, ideal Langevin; and spring-connected, inertial, nonideal Langevin cases.*

the equations of the Langevin dynamics (2.5) take the following simpler and final form (details in Appendix A), which is our "benchmark" problem suitable for analytical and numerical inspections:

$$\ddot{x} = -s_x x - 2\,(\dot{x} - ry) + \eta_x\,, \tag{2.13a}$$

$$\ddot{y} = -s_y y - 2\dot{y} + \eta_y\,, \tag{2.13b}$$

with unaltered (2.3) and with only three dimensionless parameters s_x, s_y, and r, representing the strengths of the effective springs (in the x- and y-directions) and the shear rate, respectively. We have omitted all asterisks from (2.13), and a dot here denotes a derivative with respect to the reduced time $t_* = t/t_{\rm ref}$ (2.10). All results obtained for the reduced quantities can be converted, according to (2.10), to dimensional results involving all six parameters in (2.5) by multiplying each x, y, and t by $q_{\rm ref}$, $q_{\rm ref}$, and $t_{\rm ref}$, respectively. In what follows we derive time correlation functions and other quantities of the linear Langevin dynamics (2.1) with (2.4) under various possible conditions, as illustrated in Figure 1.

3. Derivation of Time Correlation Functions. In this section, we analytically derive time correlation functions of the coupled linear Langevin dynamics (2.1) with and without inertial effects. While stationary time correlation functions exist for the case of non-purely irrotational flow, as proven in subsection 3.7, nonstationary correlation functions for the case of irrotational flow occur in subsections 3.1 and 3.3.

3.1. Ideal Brownian Dynamics: $m = 0, k_x = k_y = 0$. We first consider the ideal Brownian dynamics case where both the inertia and effective springs are absent (i.e., $m = 0$ and $k_x = k_y = 0$). In this case, the system (2.6) describes a freely diffusing massless particle in the presence of a shear flow field and includes classical Brownian motion of a particle in a quiescent background medium as a special case for $\kappa_{xy} = 0$. Since the zeroth mode in the normal coordinates [14, 15] corresponds to the center of mass of a chain, we indeed need the results of the springless case treated

Downloaded 10/30/20 to 59.64.129.2. Redistribution subject to SIAM license or copyright; see https://epubs.siam.org/page/terms

Copyright © by SIAM. Unauthorized reproduction of this article is prohibited.

Downloaded 10/30/20 to 59.64.129.2. Redistribution subject to SIAM license or copyright; see https://epubs.siam.org/page/terms

here, which are essential for transferring the results of a single harmonic oscillator to those of a bead-spring chain [29, 32] or a dumbbell (see subsection 2.1). To be more precise, the equations of motion of (2.6) in this case reduce to

$$\dot{x} = \kappa_{xy} y + \sqrt{2D}\,\eta_x\,, \tag{3.1a}$$

$$\dot{y} = \sqrt{2D}\,\eta_y\,, \tag{3.1b}$$

where D is a diffusion coefficient as confirmed by (3.4) below. Since $\langle \eta_\mu \rangle = 0$, we have $\langle \dot{y} \rangle = 0$ and $\langle \dot{x} \rangle = \kappa_{xy} \langle y \rangle$ on average. Unless otherwise stated, we assume $t \geq 0$ throughout this article, since results associated with $t < 0$ can be read off by symmetry arguments. Subject to initial conditions of $x(0) = x_0$ and $y(0) = y_0$, (3.1) are solved by

$$x(t) - x(0) = \int_0^t \dot{x}(t')\,\mathrm{d}t' = \int_0^t \left[\kappa_{xy} y(t') + \sqrt{2D}\,\eta_x(t')\right] \mathrm{d}t'\,, \tag{3.2a}$$

$$y(t) - y(0) = \int_0^t \dot{y}(t')\,\mathrm{d}t' = \sqrt{2D} \int_0^t \eta_y(t')\,\mathrm{d}t'\,. \tag{3.2b}$$

Making use of the properties of the Wiener noise (2.3), we obtain the following two-point nonstationary time correlation function:

$$\begin{aligned}
\langle [y(t_1) - y_0][y(t_2) - y_0] \rangle &= 2D \left\langle \int_0^{t_1} \eta_y(t_1')\,\mathrm{d}t_1' \int_0^{t_2} \eta_y(t_2')\,\mathrm{d}t_2' \right\rangle \\
&= 2D \int_0^{t_1} \int_0^{t_2} \langle \eta_y(t_1')\,\eta_y(t_2') \rangle\,\mathrm{d}t_2'\,\mathrm{d}t_1' \\
&= 2D \int_0^{t_1} \int_0^{t_2} \delta(t_1' - t_2')\,\mathrm{d}t_2'\,\mathrm{d}t_1' \\
&= 2D \int_0^{\min(t_1,t_2)} \int_0^{\min(t_1,t_2)} \delta(t_1' - t_2')\,\mathrm{d}t_2'\,\mathrm{d}t_1' \\
&= 2D \int_0^{\min(t_1,t_2)} \mathrm{d}t_1' = 2D \min(t_1, t_2)\,.
\end{aligned} \tag{3.3}$$

Note that result (3.3) may alternatively be obtained without making use of the properties of Dirac delta distributions, but instead via Itô isometry [51]. The famous mean squared displacement emerges as a special case of (3.3) with $t \equiv t_1 = t_2$,

$$\left\langle [y(t) - y(0)]^2 \right\rangle = 2Dt\,, \tag{3.4}$$

which actually confirms D to be a diffusion coefficient, as it is usually defined by (3.4). We can further proceed by calculating the remaining mean squared displacements (see Appendices B.1 and B.2 for proofs)

$$\langle [x(t) - x(0)][y(t) - y(0)] \rangle = D\kappa_{xy} t^2 \tag{3.5}$$

and

$$\left\langle [x(t) - x(0)]^2 \right\rangle = 2Dt \left[1 + \frac{1}{3} (\kappa_{xy} t)^2\right] + (\kappa_{xy} y_0 t)^2\,, \tag{3.6}$$

which reduces to the equilibrium result (3.4) in the absence of shear (i.e., $\kappa_{xy} = 0$). Note that the appearance of the t^3 term in (3.6) reflects the anomalous diffusion that is caused by a velocity change along the flow direction (the x-direction) due to the Brownian motion of a particle along the velocity gradient (the y-direction), and it was confirmed experimentally in [52, 61].

Copyright © by SIAM. Unauthorized reproduction of this article is prohibited.

Downloaded 10/30/20 to 59.64.129.2. Redistribution subject to SIAM license or copyright; see https://epubs.siam.org/page/terms

3.2. Nonideal Brownian Dynamics: $m = 0, k_x, k_y > 0$. We next consider the nonideal Brownian dynamics case of the oscillator with effective springs (i.e., $m = 0$ and $k_x, k_y > 0$), subject to boundary conditions $x(-\infty) = y(-\infty) = 0$. In this case, the system (2.6) is formally solved by

$$x(t) = \int_{-\infty}^{t} \left[\kappa_{xy} y(t') + \sqrt{2D}\,\eta_x(t')\right] e^{-\omega_x (t-t')}\,\mathrm{d}t' \,, \tag{3.7a}$$

$$y(t) = \sqrt{2D} \int_{-\infty}^{t} \eta_y(t') e^{-\omega_y (t-t')}\,\mathrm{d}t' \,, \tag{3.7b}$$

which may be verified by direct insertion. One has $\langle x\rangle = \langle y\rangle = 0$ on average. The stationary time correlation function $\langle y(t_1)y(t_2)\rangle$ can be obtained as (see Appendix C.1 for a proof)

$$\langle y(t_1)y(t_2)\rangle = \frac{D}{\omega_y} e^{-\omega_y |t_1 - t_2|} \,, \tag{3.8}$$

implying special cases of

$$\langle y(t)y(0)\rangle = \frac{D}{\omega_y} e^{-\omega_y t} \,, \quad \left\langle y^2 \right\rangle = \frac{D}{\omega_y} \,. \tag{3.9}$$

The remaining stationary time cross-correlation functions are derived in Appendices C.2 and C.3:

$$\langle x(t)y(0)\rangle = D\kappa_{xy}\, \frac{(\omega_x + \omega_y) e^{-\omega_y t} - 2\omega_y e^{-\omega_x t}}{(\omega_x^2 - \omega_y^2)\omega_y} \,, \tag{3.10a}$$

$$\langle y(t)x(0)\rangle = \frac{D\kappa_{xy} e^{-\omega_y t}}{(\omega_x + \omega_y)\omega_y} \,. \tag{3.10b}$$

For the stationary mixed moment we thus obtain

$$\langle xy\rangle = \frac{D\kappa_{xy}}{(\omega_x + \omega_y)\omega_y} \,, \tag{3.11}$$

and the stationary autocorrelation function in the x-direction becomes, according to Appendix C.4,

$$\langle x(t)x(0)\rangle = \frac{D e^{-\omega_x t}}{\omega_x} + \frac{D\kappa_{xy}^2 \left(\omega_x e^{-\omega_y t} - \omega_y e^{-\omega_x t}\right)}{(\omega_x^2 - \omega_y^2)\omega_x \omega_y} \,, \tag{3.12}$$

with the stationary second moment

$$\left\langle x^2 \right\rangle = \frac{D}{\omega_x} + \frac{D\kappa_{xy}^2}{(\omega_x + \omega_y)\omega_x \omega_y} \,. \tag{3.13}$$

In the case of a vanishing shear rate (i.e., $\kappa_{xy} = 0$), the system (2.6) decouples: both stationary cross-correlations $\langle x(t)y(0)\rangle$ (3.10a) and $\langle y(t)x(0)\rangle$ (3.10b) vanish, and $\langle x(t)x(0)\rangle$ (3.12) reduces to $\langle y(t)y(0)\rangle$ (3.9). Finally, we list the stationary time correlation functions in the special case of pure shear, $\omega \equiv \omega_x = \omega_y$ (i.e., for an

Copyright © by SIAM. Unauthorized reproduction of this article is prohibited.

Downloaded 10/30/20 to 59.64.129.2. Redistribution subject to SIAM license or copyright; see https://epubs.siam.org/page/terms

oscillator in the absence of elongational flow components), in which neither (3.10a) nor (3.12) diverges:

(3.14a)
$$\langle y(t)y(0)\rangle = \frac{De^{-\omega t}}{\omega} = \frac{k_{\mathrm{B}}T}{k}e^{-kt/\gamma}\,,$$

(3.14b)
$$\langle x(t)y(0)\rangle = \frac{D\kappa_{xy}\,(1+2\omega t)\,e^{-\omega t}}{2\omega^2} = \frac{k_{\mathrm{B}}T\kappa_{xy}}{2k^2}\,(\gamma+2kt)\,e^{-kt/\gamma} = \langle y(-t)x(0)\rangle\,,$$

(3.14c)
$$\langle y(t)x(0)\rangle = \frac{D\kappa_{xy}e^{-\omega t}}{2\omega^2} = \frac{k_{\mathrm{B}}T\gamma\kappa_{xy}}{2k^2}e^{-kt/\gamma} = \langle x(-t)y(0)\rangle\,,$$

(3.14d)
$$\langle x(t)x(0)\rangle = \frac{De^{-\omega t}}{\omega} + \frac{D\kappa_{xy}^2\,(1+\omega t)\,e^{-\omega t}}{2\omega^3} = \frac{k_{\mathrm{B}}T}{2k^3}\left(2k^2+\gamma^2\kappa_{xy}^2+\gamma\kappa_{xy}^2kt\right)e^{-kt/\gamma}\,.$$

More specifically, the stationary moments are read off at $t=0$,

(3.15)
$$\left\langle y^2\right\rangle = \frac{D}{\omega} = \frac{k_{\mathrm{B}}T}{k}\,,\quad \langle xy\rangle = \frac{D\kappa_{xy}}{2\omega^2} = \frac{k_{\mathrm{B}}T\gamma\kappa_{xy}}{2k^2}\,,\quad \left\langle x^2\right\rangle = \frac{D}{\omega}+\frac{D\kappa_{xy}^2}{2\omega^3} = \frac{k_{\mathrm{B}}T}{k}+\frac{k_{\mathrm{B}}T\gamma^2\kappa_{xy}^2}{2k^3}\,.$$

We can furthermore derive the mean squared displacement in the y-direction,

$$\left\langle [y(t)-y(0)]^2\right\rangle = 2\left\langle y^2\right\rangle - 2\,\langle y(t)y(0)\rangle = 2Dt + O(t^2)\,, \tag{3.16}$$

which indicates that the mean squared displacement is linear in t only at small times, which qualitatively differs from what we derived for the noninertial case, (3.4), in subsection 3.1. In the limit of vanishing effective springs, however, the mean squared displacement (3.16) reduces to (3.4), since $k^{-1}[1-\exp(-\alpha k)] = \alpha + O(k)$.

3.3. Ideal Langevin Dynamics: $m > 0, k_x = k_y = 0$. We next consider the ideal Langevin dynamics case of a free particle, an oscillator without effective springs (i.e., $m > 0$ and $k_x = k_y = 0$) [17]. In this case, the dimensionless (2.13) takes the form

$$\ddot{x} = -2(\dot{x} - ry) + \eta_x\,, \tag{3.17a}$$
$$\ddot{y} = -2\dot{y} + \eta_y\,, \tag{3.17b}$$

for which one is mostly interested in mean squared displacements rather than time correlation functions, since the latter depend on the initial conditions. In the absence of shear, both components are independent of each other, and only velocities rather than coordinates appear in the equations of motion. By comparing (3.17) with (2.6) and (3.7), we have

$$\dot{x}(t) = \int_{-\infty}^{t} [2ry(t') + \eta_x(t')]\,e^{-2(t-t')}\,\mathrm{d}t'\,, \tag{3.18a}$$
$$\dot{y}(t) = \int_{-\infty}^{t} \eta_y(t')e^{-2(t-t')}\,\mathrm{d}t'\,, \tag{3.18b}$$

where $\dot{x}$ and $\dot{y}$ have the interpretation of the velocities. We can read off the stationary velocity autocorrelation function and the mean squared displacement, respectively,

Copyright © by SIAM. Unauthorized reproduction of this article is prohibited.

Downloaded 10/30/20 to 59.64.129.2. Redistribution subject to SIAM license or copyright; see https://epubs.siam.org/page/terms

from (3.8)–(3.9) upon inspecting the case of $D = 1/2$ and $\omega_y = 2$ in (3.7b). This yields

$$\langle \dot{y}(t)\dot{y}(0)\rangle = \frac{1}{4}e^{-2t}\,, \tag{3.19}$$

and, as shown in Appendix D.1,

$$\left\langle [y(t) - y(0)]^2 \right\rangle = \frac{1}{8}\left(2t + e^{-2t} - 1\right)\,. \tag{3.20}$$

Redimensionalizing (3.19) the more familiar version of the dimensional velocity autocorrelation function arises:

$$\langle \dot{y}(t)\dot{y}(0)\rangle = \frac{k_{\mathrm{B}}T}{m}e^{-\gamma t/m}\,. \tag{3.21}$$

In this ideal (free, springless, $k = 0$) case, the integrated velocity autocorrelation function turns out to be the diffusion coefficient,

$$\int_0^\infty \langle \dot{y}(t)\dot{y}(0)\rangle \,\mathrm{d}t = D \equiv \frac{k_{\mathrm{B}}T}{\gamma}\,. \tag{3.22}$$

Similarly, redimensionalizing (3.20) yields the dimensional mean squared displacement,

$$\left\langle [y(t) - y(0)]^2 \right\rangle = \frac{2mk_{\mathrm{B}}T}{\gamma^2}\left(\gamma t/m + e^{-\gamma t/m} - 1\right) = \frac{k_{\mathrm{B}}T}{m}t^2 + O(t^3)\,. \tag{3.23}$$

While this expression is quadratic in t at small times, it reaches $2Dt$ (the diffusive regime) for large times (i.e., $\gamma t/m \gg 1$). A similar calculation, where the boundary condition plays a role as in subsection 3.1, can be performed to obtain the mean squared displacement in the x-direction. The mean squared velocity $\langle \dot{y}^2\rangle = k_{\mathrm{B}}T/m$ (3.21) is in agreement with the equipartition theorem here, in sharp contrast with Brownian dynamics, in which $\langle \dot{y}^2\rangle = 2D\delta(0)$ involves the diverging Dirac delta distribution.

3.4. Nonideal Langevin Dynamics: $m > 0, k \equiv k_x = k_y > 0$. We finally consider the most general nonideal Langevin dynamics case with both inertia and effective springs (i.e., $m > 0$ and $k \equiv k_x = k_y > 0$). For the sake of simplicity we assume $s \equiv s_x = s_y$ in this case, and the equations of motion of the dimensionless system (2.13) read

$$\ddot{x} = -sx - 2(\dot{x} - ry) + \eta_x\,, \tag{3.24a}$$

$$\ddot{y} = -sy - 2\dot{y} + \eta_y\,. \tag{3.24b}$$

As demonstrated in Appendix E.1, the solution of (3.24b) subject to the initial conditions of $y(-\infty) = 0$ and $\dot{y}(-\infty) = 0$ appropriate for the calculation of correlation functions is given by

$$y(t) = \frac{1}{2\sqrt{1-s}}\left[G_y(t, s_-) - G_y(t, s_+)\right]\,, \tag{3.25}$$

where

$$G_y(t, s') \equiv \int_{-\infty}^{t} e^{-s'(t-t')}\,\eta_y(t')\,\mathrm{d}t'\,, \tag{3.26}$$

Copyright © by SIAM. Unauthorized reproduction of this article is prohibited.

with the abbreviation

$$s_\pm = 1 \pm \sqrt{1-s}\,. \tag{3.27}$$

Similarly, we can also obtain the solution of (3.24a) as

$$x(t) = \frac{1}{2\sqrt{1-s}}\left[G_x(t,s_-) - G_x(t,s_+)\right], \tag{3.28}$$

where

$$G_x(t,s') \equiv \int_{-\infty}^{t} e^{-s'(t-t')}\left[2ry(t') + \eta_x(t')\right]\mathrm{d}t'\,. \tag{3.29}$$

Subsequently, we can derive a variety of dimensionless, stationary time correlation functions as in subsection 3.2 (details of derivations in Appendices E.2 to E.5):

$$\langle y(t)y(0)\rangle = \frac{C_1^+ + C_1^-}{8s\sqrt{1-s}}\,, \tag{3.30a}$$

$$\langle x(t)y(0)\rangle = \frac{r\left(A^+ - A^-\right)}{8s^2(1-s)^{3/2}} = \langle y(-t)x(0)\rangle\,, \tag{3.30b}$$

$$\langle y(t)x(0)\rangle = \frac{r\left(C_2^- - C_2^+\right)}{16s^2\sqrt{1-s}} = \langle x(-t)y(0)\rangle\,, \tag{3.30c}$$

$$\langle x(t)x(0)\rangle = \frac{C_1^+ + C_1^-}{8s\sqrt{1-s}} + \frac{r^2\left(B^+ + B^-\right)}{16s^3(1-s)^{3/2}}\,, \tag{3.30d}$$

with the dimensionless, reduced time-dependent coefficients

$$A^\pm = \left[1 + \left(\frac{1}{2}+t\right)(1-s) \pm (2+t)\sqrt{1-s}\right] C_2^\pm\,, \tag{3.31a}$$

$$B^\pm = \left[\sqrt{1-s}\,(st+s+1) \pm (2s-1)\right] C_2^\pm\,, \tag{3.31b}$$

$$C_n^\pm = \left(\sqrt{1-s} \mp 1\right)^n \exp\left[-\left(1 \pm \sqrt{1-s}\right)t\right]. \tag{3.31c}$$

More specifically, for $t = 0$, (3.30) becomes

$$\left\langle y^2\right\rangle = \frac{1}{4s}\,, \quad \langle xy\rangle = \frac{r}{4s^2}\,, \quad \left\langle x^2\right\rangle = \frac{1}{4s} + \frac{r^2(s+4)}{8s^3}\,. \tag{3.32}$$

As in subsection 3.2, in the case of a vanishing shear rate (i.e., $\kappa_{xy} = 0$ and subsequently $r = 0$), the system (3.24) decouples: both cross-correlations $\langle x(t)y(0)\rangle$ (3.30b) and $\langle y(t)x(0)\rangle$ (3.30c) vanish, and $\langle x(t)x(0)\rangle$ (3.30d) reduces to $\langle y(t)y(0)\rangle$ (3.30a), which can be rewritten as

$$\langle y(t)y(0)\rangle = \frac{1}{4s}\left[\cosh(t\sqrt{1-s}) + \frac{\sinh(t\sqrt{1-s})}{\sqrt{1-s}}\right] e^{-t}\,. \tag{3.33}$$

Redimensionalizing (3.33) yields the dimensional, stationary time correlation function

$$\langle y(t)y(0)\rangle = \frac{k_\mathrm{B}T}{k}\left[\cosh(\nu t) + \frac{\gamma}{2m\nu}\sinh(\nu t)\right] e^{-\gamma t/2m}\,, \tag{3.34}$$

where

$$\nu = \sqrt{\gamma^2/4m^2 - k/m}\,, \tag{3.35}$$

Copyright © by SIAM. Unauthorized reproduction of this article is prohibited.

Downloaded 10/30/20 to 59.64.129.2. Redistribution subject to SIAM license or copyright; see https://epubs.siam.org/page/terms

Downloaded 10/30/20 to 59.64.129.2. Redistribution subject to SIAM license or copyright; see https://epubs.siam.org/page/terms

which is in perfect agreement with the dimensional result of [65]. More specifically, $\langle y^2 \rangle$ can be obtained alternatively via the Gibbs–Boltzmann distribution, given $U(y) = ky^2/2$ for the harmonic oscillator:

$$\langle y^2 \rangle = \frac{\int_{-\infty}^{\infty} y^2 \exp[-U(y)/k_{\mathrm{B}}T]\,\mathrm{d}y}{\int_{-\infty}^{\infty} \exp[-U(y)/k_{\mathrm{B}}T]\,\mathrm{d}y} = \frac{k_{\mathrm{B}}T}{k}\,. \tag{3.36}$$

We can furthermore derive the mean squared displacement of

$$\left\langle [y(t) - y(0)]^2 \right\rangle = 2\left\langle y^2 \right\rangle - 2\left\langle y(t)y(0) \right\rangle = \frac{k_{\mathrm{B}}T}{m}\left(1 - \frac{\gamma^2}{4mk}\right) t^2 + O(t^3)\,, \tag{3.37}$$

which indicates that the mean squared displacement is quadratic in t at small times.

3.5. Connection between Noninertial and Inertial Results. To demonstrate that the noninertial results of the stationary time correlation functions in subsection 3.2 are special cases (i.e., in the limit of vanishing mass) of the results with inertia in subsection 3.4, we have to first write down the time correlation functions (3.30) using dimensional quantities. To this end we reintroduce the original dimensional variables m, k, γ, σ, $k_{\mathrm{B}}T$, κ_{xy}, and t. This is done by multiplying each time correlation function by q_{ref}^2 and subsequently replacing $t \to t/t_{\mathrm{ref}}$ and expanding s and r using the definitions in (2.12). Throughout this subsection, $\to$ stands for "going from dimensionless to dimensional." By performing Taylor series expansions in m around $m = 0$, we obtain some helpful intermediate results:

$$\frac{q_{\mathrm{ref}}^2}{8s\sqrt{1-s}} \;\to\; \frac{k_{\mathrm{B}}T}{2k\sqrt{1-4mk/\gamma^2}} = \frac{k_{\mathrm{B}}T}{2k} + O(m)\,, \tag{3.38a}$$

$$\frac{rq_{\mathrm{ref}}^2}{8s^2(1-s)^{3/2}} \;\to\; \frac{k_{\mathrm{B}}T\gamma\kappa_{xy}}{4k^2} + O(m)\,, \tag{3.38b}$$

$$\frac{rq_{\mathrm{ref}}^2}{16s^2\sqrt{1-s}} \;\to\; \frac{k_{\mathrm{B}}T\gamma\kappa_{xy}}{8k^2} + O(m)\,, \tag{3.38c}$$

$$\frac{r^2q_{\mathrm{ref}}^2}{16s^3(1-s)^{3/2}} \;\to\; \frac{k_{\mathrm{B}}T\gamma^2\kappa_{xy}^2}{16k^3} + O(m)\,, \tag{3.38d}$$

as well as

$$(\mp s_{\mp})^n \to (1 \mp 1)^n - \frac{2n(1 \mp 1)^{n-1}}{\gamma^2/mk} \pm \frac{2n(1 \mp 1)^{n-2}[1 \pm (n-2)]}{(\gamma^2/mk)^2} + O(m^3)\,, \tag{3.39a}$$

$$s_{\pm}t \to \frac{\gamma t}{2m}\left(1 \pm \sqrt{1 - 4mk/\gamma^2}\right) = \mp\frac{kt}{\gamma}\left(1 + \frac{mk}{\gamma^2}\right) + (1 \pm 1)\,\frac{\gamma t}{2m} + O(m^2), \tag{3.39b}$$

where t on the left-hand side in (3.39b) is the dimensionless time, whereas t on the right-hand side denotes the dimensional time. For small m (and $n > 0$), (3.39) implies

$$(+s_+)^n \;\to\; 2^n + O(m)\,, \tag{3.40a}$$

$$(-s_-)^n \;\to\; O(m^n)\,, \tag{3.40b}$$

$$e^{-s_+t} \;\to\; e^{-\gamma t/m}\,, \tag{3.40c}$$

$$e^{-s_-t} \;\to\; e^{-kt/\gamma} + O(m)\,, \tag{3.40d}$$

Copyright © by SIAM. Unauthorized reproduction of this article is prohibited.

Downloaded 10/30/20 to 59.64.129.2. Redistribution subject to SIAM license or copyright; see https://epubs.siam.org/page/terms

where we have kept $\exp(-\gamma t/m)$ as it cannot be Taylor expanded; it asymptotically vanishes in the limit $m \to 0$ as long as $\gamma t > 0$. We recall from (3.31c) that the coefficients $C_n^{\pm}$ are given by $C_n^{\pm} = (\mp s_{\mp})^n e^{-s_{\pm} t}$. With the help of (3.40), we find

$$C_n^+ = (-s_-)^n e^{-s_+ t} \;\to\; O(m^n) e^{-\gamma t/m}\,, \tag{3.41a}$$

$$C_n^- = (+s_+)^n e^{-s_- t} \;\to\; 2^n e^{-kt/\gamma} + O(m)\,, \tag{3.41b}$$

and thus only the coefficients C_n^- survive in the limit of vanishing m,

$$\lim_{m\to 0} \langle y(t) y(0)\rangle \;\to\; \lim_{m\to 0} \frac{q_{\mathrm{ref}}^2 (C_1^+ + C_1^-)}{8s\sqrt{1-s}} = \frac{k_{\mathrm{B}}T}{k} e^{-kt/\gamma}\,, \tag{3.42a}$$

$$\lim_{m\to 0} \langle y(t) x(0)\rangle \;\to\; \lim_{m\to 0} \frac{q_{\mathrm{ref}}^2 r (C_2^- - C_2^+)}{16 s^2 \sqrt{1-s}} = \frac{k_{\mathrm{B}}T\gamma\kappa_{xy}}{2k^2} e^{-kt/\gamma}\,, \tag{3.42b}$$

where (3.38a) and (3.38c) have been used. Equations (3.42a) and (3.42b) coincide with the results (3.14a) and (3.14c) obtained by a direct calculation with $m = 0$. To calculate the remaining two correlations, we begin with two intermediate results that both follow from (3.31),

$$\begin{aligned} \frac{A^{\pm}}{C_2^{\pm}} &\;\to\; 1 + \left(\frac{1}{2} + \frac{\gamma t}{2m}\right)\left(1 - \frac{4mk}{\gamma^2}\right) \pm \left(2 + \frac{\gamma t}{2m}\right)\sqrt{1 - \frac{4mk}{\gamma^2}} \\ &= (1 \pm 1)\,\frac{\gamma t}{2m} + \frac{3}{2} \pm 2 - (2 \pm 1)\,\frac{kt}{\gamma} + O(m)\,, \end{aligned} \tag{3.43a}$$

$$\begin{aligned} \frac{B^{\pm}}{C_2^{\pm}} &\;\to\; \sqrt{1 - \frac{4mk}{\gamma^2}}\left(\frac{2kt}{\gamma} + \frac{4mk}{\gamma^2} + 1\right) \pm \left(\frac{8mk}{\gamma^2} - 1\right) \\ &= (1 \mp 1) + \frac{2kt}{\gamma} + O(m)\,. \end{aligned} \tag{3.43b}$$

Since $m^{-1} C_n^+$ vanishes according to (3.41a) as $O(m^{n-1}) e^{-\gamma t/m}$, both A^+ and B^+ vanish in the limit of vanishing mass, and the remaining A^- and B^- are

$$A^- \;\to\; \left(\frac{3}{2} - 2 - \frac{kt}{\gamma}\right) 2^2 e^{-kt/\gamma} + O(m)\,, \tag{3.44a}$$

$$B^- \;\to\; \left(2 + \frac{2kt}{\gamma}\right) 2^2 e^{-kt/\gamma} + O(m)\,, \tag{3.44b}$$

such that we find, with the help of (3.38b), (3.38d), (3.43a), and (3.43b),

$$\lim_{m\to 0} \langle x(t) y(0)\rangle \;\to\; \lim_{m\to 0} \frac{q_{\mathrm{ref}}^2 r\,(A^+ - A^-)}{8 s^2 (1-s)^{3/2}} = \frac{k_{\mathrm{B}}T\kappa_{xy}}{2k^2}\,(\gamma + 2kt)\, e^{-kt/\gamma}\,, \tag{3.45a}$$

$$\begin{aligned} \lim_{m\to 0} \langle x(t) x(0)\rangle &\;\to\; \lim_{m\to 0} \langle y(t) y(0)\rangle + \lim_{m\to 0} \frac{q_{\mathrm{ref}}^2 r^2\,(B^+ + B^-)}{16 s^3 (1-s)^{3/2}} \\ &= \frac{k_{\mathrm{B}}T}{2k^3}\left(2k^2 + \gamma^2\kappa_{xy}^2 + \gamma\kappa_{xy}^2 kt\right) e^{-kt/\gamma}\,, \end{aligned} \tag{3.45b}$$

in complete agreement with the results obtained by the direct calculation with $m = 0$, (3.14b) and (3.14d), respectively.

Copyright © by SIAM. Unauthorized reproduction of this article is prohibited.

Downloaded 10/30/20 to 59.64.129.2. Redistribution subject to SIAM license or copyright; see https://epubs.siam.org/page/terms

3.6. Alternative Approach via Fourier Transform. We have demonstrated in subsection 3.4 how the time correlation functions for the most general nonideal Langevin dynamics case can be derived via a direct approach, where the Dirac delta distribution is eliminated by integrating over it. In this subsection, we outline an alternative approach utilizing Fourier transforms, which is related to the Wiener–Khinchin theorem. In this case, we eliminate the Dirac delta distribution by noting that $\delta(t)$ is the inverse Fourier-transformed "one" (see (3.49) below). In what follows we demonstrate how this alternative approach works only in an example of the stationary time correlation function of $\langle y(t)y(0)\rangle$ (3.30a). Upon substituting $t-t'$ by t_1, we can rewrite (3.25) more conveniently as

$$\begin{aligned} y(t) &= \frac{1}{\sqrt{1-s}} \int_{-\infty}^{t} \sinh\left[(t-t')\sqrt{1-s}\right] e^{-\left(t-t'\right)} \eta_y(t')\,\mathrm{d}t' \\ &= \frac{1}{\sqrt{1-s}} \int_{0}^{\infty} \sinh\left[t_1\sqrt{1-s}\right] e^{-t_1} \eta_y(t-t_1)\,\mathrm{d}t_1 \\ &= \int_{0}^{\infty} \Omega_{t_1}\, \eta_y(t-t_1)\,\mathrm{d}t_1\,, \end{aligned} \tag{3.46}$$

with a weighting function Ω defined as

$$\Omega_\nu \equiv \frac{e^{-\nu}\sinh(\nu\sqrt{1-s})}{\sqrt{1-s}} = \begin{cases} (1-s)^{-1/2}e^{-\nu}\sinh(\nu\sqrt{1-s})\,, & s \le 1\,, \\ (s-1)^{-1/2}e^{-\nu}\sin(\nu\sqrt{s-1})\,, & s > 1\,, \end{cases} \tag{3.47}$$

where we have also mentioned the purely real-valued version for $s > 1$. Now making use of the Fourier transform

$$\mathrm{FT}\{f(p)\}(t) = \frac{1}{\sqrt{2\pi}} \int_{-\infty}^{\infty} f(p) e^{ipt}\,\mathrm{d}p\,, \tag{3.48}$$

as well as a basic identity that should be regarded as an equality in the sense of tempered distributions,

$$\delta(t) = \frac{1}{2\pi} \int_{-\infty}^{\infty} e^{ipt}\,\mathrm{d}p = \frac{1}{\sqrt{2\pi}}\,\mathrm{FT}\left\{1\right\}(t)\,, \tag{3.49}$$

the stationary time correlation function of $\langle y(t)y(0)\rangle$ (3.30a) can be recalculated as

$$\begin{aligned} \langle y(t)y(0)\rangle &= \int_0^\infty \int_0^\infty \Omega_{t_1}\Omega_{t_2} \left\langle \eta_y(t-t_1)\eta_y(0-t_2)\right\rangle \mathrm{d}t_2\,\mathrm{d}t_1 \\ &= \int_0^\infty \int_0^\infty \Omega_{t_1}\Omega_{t_2} \delta(t-t_1+t_2)\,\mathrm{d}t_2\,\mathrm{d}t_1 \\ &= \frac{1}{2\pi}\int_{-\infty}^{\infty} \left[\int_0^\infty \int_0^\infty \Omega_{t_1}\Omega_{t_2} e^{ip(t-t_1+t_2)}\,\mathrm{d}t_2\,\mathrm{d}t_1\right]\mathrm{d}p \\ &= \frac{1}{2\pi}\int_{-\infty}^{\infty} \frac{e^{ipt}}{p^4 - 2p^2(s-2)+s^2}\,\mathrm{d}p \\ &= \frac{1}{\sqrt{2\pi}}\,\mathrm{FT}\left\{\frac{1}{p^4-2p^2(s-2)+s^2}\right\}(t) \\ &= \frac{1}{4s}\left[\cosh(t\sqrt{1-s}) + \frac{\sinh(t\sqrt{1-s})}{\sqrt{1-s}}\right] e^{-t} = \frac{C_1^+ + C_1^-}{8s\sqrt{1-s}}\,. \end{aligned} \tag{3.50}$$

The remaining stationary time correlation functions in subsection 3.4 can be similarly obtained, although the calculations are more involved.

Copyright © by SIAM. Unauthorized reproduction of this article is prohibited.

Downloaded 10/30/20 to 59.64.129.2. Redistribution subject to SIAM license or copyright; see https://epubs.siam.org/page/terms

3.7. Alternative Approach via Fokker–Planck Equation. A complementary approach to the moments and stationary correlation functions is based on the equivalence between the Langevin dynamics for a stochastic variable $\mathbf{Q}(t)$ and a Fokker–Planck equation for the probability distribution function $f(\mathbf{Q},t)$. The Fokker–Planck equation corresponding to the Langevin dynamics in its rather general form

$$\dot{\mathbf{Q}} = \mathbf{a} + \frac{1}{2}\nabla\cdot\mathbf{D} + \mathbf{B}\cdot\boldsymbol{\eta}\,, \qquad \nabla = \frac{\partial}{\partial\mathbf{Q}}\,, \tag{3.51}$$

with $\mathbf{Q}$- and t-dependent vector $\mathbf{a}$, and matrices $\mathbf{B}$ and $\mathbf{D} = \mathbf{B}\cdot\mathbf{B}^{\mathrm{T}}$, fulfills the Fokker–Planck equation

$$\frac{\partial f}{\partial t} = -\nabla\cdot(\mathbf{a}f) + \frac{1}{2}\nabla\cdot(\mathbf{D}\cdot\nabla f)\,. \tag{3.52}$$

In view of (4.6) the benchmark Langevin dynamics (2.13) is of the form (3.51) with $\mathbf{a} = -\mathbf{A}\cdot\mathbf{Q}$ and constant matrices $\mathbf{A}$ and $\mathbf{B}$,

$$\mathbf{A} = \begin{pmatrix} 0 & 0 & -1 & 0 \\ 0 & 0 & 0 & -1 \\ s_x & -2r & 2 & 0 \\ 0 & s_y & 0 & 2 \end{pmatrix}, \qquad \mathbf{B} = \begin{pmatrix} \mathbf{0} & \mathbf{0} \\ \mathbf{0} & \mathbf{I} \end{pmatrix}, \tag{3.53}$$

while $\mathbf{Q}$ is the four-dimensional vector $(\mathbf{q}, \mathbf{p} = m\dot{\mathbf{q}})$. With $\mathbf{Y}(t) = \exp[-\mathbf{A}t]$ the time evolution of the mean value is $\langle\mathbf{Q}\rangle(t) = \mathbf{Y}\cdot\mathbf{Q}_0$ and the variance $\boldsymbol{\Sigma} = \langle\mathbf{Q}\mathbf{Q}\rangle - \langle\mathbf{Q}\rangle\langle\mathbf{Q}\rangle$ fulfills [25]

$$\dot{\boldsymbol{\Sigma}} = -\left[\mathbf{A}\cdot\boldsymbol{\Sigma} + \boldsymbol{\Sigma}\cdot\mathbf{A}^{\mathrm{T}}\right] + \mathbf{D}\,. \tag{3.54}$$

With $\boldsymbol{\Sigma}(t)$ at hand the solution of the Fokker–Planck equation (3.52) subject to the initial condition $p(\mathbf{Q},0) = \delta(\mathbf{Q}-\mathbf{Q}_0)$ reads

$$p(\mathbf{Q},t) = \frac{1}{(2\pi)\sqrt{|\boldsymbol{\Sigma}(t)|}}\exp\left\{-\frac{1}{2}\left[\mathbf{Q}-\langle\mathbf{Q}\rangle(t)\right]^{\mathrm{T}}\cdot\boldsymbol{\Sigma}^{-1}(t)\cdot\left[\mathbf{Q}-\langle\mathbf{Q}\rangle(t)\right]\right\}, \tag{3.55}$$

and a stationary solution exists if (3.54) has a solution for $\dot{\boldsymbol{\Sigma}} = \mathbf{0}$, denoted by $\boldsymbol{\Sigma}_\infty$. From the spectrum of the Fokker–Planck operator, which is the operator on the right-hand side of (3.52), one can conclude the convergence of arbitrary initial conditions to a unique equilibrium probability distribution. For the special case $s \equiv s_x = s_y$ considered earlier in subsection 3.4, the eigenvalues of $\mathbf{A}$ are $s_\pm$ (both twice degenerated), and the eigenvectors are $(-s_+/s, 0, 1, 0)$, $\mathbf{0}$, $(-s_-/s, 0, 1, 0)$, and $\mathbf{0}$, respectively. The eigenvalues are real-valued and semipositive for $s \in [0,1]$, and become complex-valued for $s > 1$, recalling $s_\pm = 1 \pm \sqrt{1-s}$. Solving the linear system of equations (3.54) (with $\dot{\boldsymbol{\Sigma}} = \mathbf{0}$) for $\boldsymbol{\Sigma}_\infty$, we then obtain

$$\boldsymbol{\Sigma}_\infty = \begin{pmatrix} \frac{2s^2+(4+s)r^2}{8s^3} & \frac{r}{4s^2} & 0 & -\frac{r}{8s} \\ \frac{r}{4s^2} & \frac{1}{4s} & \frac{r}{8s} & 0 \\ 0 & \frac{r}{8s} & \frac{1}{8}\left(2+\frac{r^2}{s}\right) & 0 \\ -\frac{r}{8s} & 0 & 0 & \frac{1}{4} \end{pmatrix}. \tag{3.56}$$

Since a stationary $\boldsymbol{\Sigma}$ exists for $s \neq 0$, the stationary distribution function is given by (3.55) with $\boldsymbol{\Sigma}(t)$ being replaced by $\boldsymbol{\Sigma}_\infty$, implying that stationary moments and

Copyright © by SIAM. Unauthorized reproduction of this article is prohibited.

Downloaded 10/30/20 to 59.64.129.2. Redistribution subject to SIAM license or copyright; see https://epubs.siam.org/page/terms

a stationary correlation function exist for $s \neq 0$. The analogous calculation for the more general case of $s_x \neq s_y$ yields that $\mathbf{\Sigma}_\infty$ exists as long as all s_μ do not vanish. For $t > 0$, the stationary correlation functions are given by

$$\langle \mathbf{Q}(t)\mathbf{Q}(0)\rangle_{\text{stat}} = e^{-\mathbf{A}t} \cdot \mathbf{\Sigma}_\infty \,, \tag{3.57a}$$

$$\langle \mathbf{Q}(0)\mathbf{Q}(t)\rangle_{\text{stat}} = \mathbf{\Sigma}_\infty \cdot e^{-\mathbf{A}^{\mathrm{T}}t} \,. \tag{3.57b}$$

For the spectral density [20],

$$\mathbf{S}(\omega) = \int_{-\infty}^{\infty} \langle \mathbf{Q}(t+\tau)\mathbf{Q}(t)\rangle_{\text{stat}} e^{-i\omega t}\, \mathrm{d}\tau = (\mathbf{A} + i\omega\mathbf{I})^{-1} \cdot \mathbf{D} \cdot \left(\mathbf{A}^{\mathrm{T}} - i\omega\mathbf{I}\right)^{-1} , \tag{3.58}$$

the situation is particularly simple as it involves only $\mathbf{A}$ and $\mathbf{D}$, but not $\mathbf{\Sigma}_\infty$. With the help of the aforementioned eigensystem of $\mathbf{A}$, we have verified that (3.57a) agrees with (3.30a).

4. Numerical Methods. In this section, we first briefly introduce the concept of the order of convergence associated with numerical methods for SDEs, followed by descriptions of numerical methods used to simulate the linear Langevin dynamics (2.1) in both the noninertial and the inertial cases. Interested readers are referred to standard textbooks [28, 36, 48] for a more thorough discussion of mathematical issues (e.g., ergodicity) of SDEs.

4.1. Order of Convergence. Numerical analysis of SDEs is typically based on the concept of *strong* and *weak* errors. We denote the stochastic solution of an SDE as $X(\tau)$ and its associated numerical approximation, with an integration timestep of h, in the form of a discrete stochastic process as $X^{n+1} = \Phi(X^n, h)$, $n = 0, 1, \ldots, N-1$, with $Nh = T$ being fixed. A method is then said to have strong order of p if there exists a constant C_1 such that

$$\mathrm{Err}_h^{\text{strong}} = \mathbb{E}|X^n - X(\tau)| \leq C_1 h^p \tag{4.1}$$

for any fixed $\tau = nh \in [0, T]$ with h being sufficiently small. The strong order of convergence (4.1) measures the rate of decay of the "mean of the error" [22], whose type of convergence is path dependent. Alternatively, one could measure the rate of decay of the "error of the means," which is related to the (weak) convergence in distribution (i.e., in approximating the expectations of the Itô process). Thus, a method is said to have weak order of p if there exists a constant C_2 such that for all suitable test functions (observables) ϕ,

$$\mathrm{Err}_h^{\text{weak}} = |\mathbb{E}\phi(X^n) - \mathbb{E}\phi(X(\tau))| \;\leq\; C_2 h^p \tag{4.2}$$

for any fixed $\tau = nh \in [0, T]$ with h being sufficiently small. It should be noted that methods with high strong order would lead to high weak order; however, the converse is in general false [36]. Since the focus of this article is on the computation of averages, the concept of weak order is rendered more appropriate.

4.2. Brownian Dynamics. We consider the linear Langevin dynamics with effective springs but without inertia described in subsection 3.2 (i.e., (2.6)), which is also known as Brownian dynamics,

$$\dot{\mathbf{q}} = -k\mathbf{q}/\gamma + \mathbf{u} + \sqrt{2D}\,\boldsymbol{\eta}\,, \tag{4.3}$$

where $\mathbf{u} = \boldsymbol{\kappa} \cdot \mathbf{q}$ is the streaming velocity field with $\boldsymbol{\kappa}$ being defined in (2.4).

Copyright © by SIAM. Unauthorized reproduction of this article is prohibited.

Downloaded 10/30/20 to 59.64.129.2. Redistribution subject to SIAM license or copyright; see https://epubs.siam.org/page/terms

4.2.1. The Euler–Maruyama (EM) Method. A simple and popular numerical method for a system of Itô SDEs is the Euler–Maruyama (EM) method, which reads

$$\mathbf{q}^{n+1} = \mathbf{q}^n - hk\mathbf{q}^n/\gamma + h\mathbf{u}^n + \sqrt{2Dh}\mathbf{R}^n\,, \tag{4.4}$$

where $\mathbf{R}^n$, resampled at each step, is a dimensionless vector whose components are drawn randomly and independently from a Gaussian probability distribution function with zero mean and unit variance, $\langle \mathbf{R}^n \mathbf{R}^m \rangle = \mathbf{I}\delta_{n,m}$; thus $\mathbf{R}^n/\sqrt{h}$ replaces the continuous $\boldsymbol{\eta}$ in a time-discrete implementation.

4.2.2. The Limit Method. A simple modification of the EM method (4.4) leads to the limit method [34]

$$\mathbf{q}^{n+1} = \mathbf{q}^n - hk\mathbf{q}^n/\gamma + h\mathbf{u}^n + \sqrt{Dh/2}\left(\mathbf{R}^n + \mathbf{R}^{n+1}\right)\,, \tag{4.5}$$

where $\mathbf{R}^n$ and $\mathbf{R}^{n+1}$ are vectors of independent Gaussian white noise with zero mean and unit variance, and it should be noted that $\mathbf{R}^{n+1}$ will become $\mathbf{R}^n$ in the subsequent step. It has been shown that such a simple modification could lead to an extra order of weak convergence [38] as well as substantial improvements in sampling accuracy [34]. Note that although the limit method was first derived from the BAOAB method introduced in subsection 4.3.2 in the large friction limit [34], it can also be obtained using postprocessed integrators [64].

4.3. Langevin Dynamics. We also consider the most general case of the linear Langevin dynamics with both inertia and effective springs described in subsection 3.4. Rewriting (3.24) in a more general and first order form yields

$$\dot{\mathbf{q}} = \mathbf{p}\,, \tag{4.6a}$$

$$\dot{\mathbf{p}} = -s\mathbf{q} - 2\left(\mathbf{p} - \mathbf{u}\right) + \boldsymbol{\eta}\,, \tag{4.6b}$$

where $\mathbf{p}$ has the interpretation of the momentum, and (4.6) can be considered as the adimensional version of (2.1), using the reference quantities (2.11) and dimensionless parameters (2.12).

4.3.1. The Stochastic Velocity Verlet (SVV) Method. Building on the popular Verlet method in molecular dynamics, and also due to its ease of implementation, the stochastic velocity Verlet (SVV) method [47] is a popular scheme for Langevin dynamics, whose integration steps read

$$\mathbf{p}^{n+1/2} = \mathbf{p}^n - hs\mathbf{q}^n/2 - h\left(\mathbf{p}^n - \mathbf{u}^n\right) + \sqrt{h/2}\mathbf{R}^n\,, \tag{4.7a}$$

$$\mathbf{q}^{n+1} = \mathbf{q}^n + h\mathbf{p}^{n+1/2}\,, \tag{4.7b}$$

$$\mathbf{p}^{n+1} = \mathbf{p}^{n+1/2} - hs\mathbf{q}^{n+1}/2 - h\left(\mathbf{p}^{n+1/2} - \mathbf{u}^{n+1}\right) + \sqrt{h/2}\mathbf{R}^{n+1/2}\,, \tag{4.7c}$$

where $\mathbf{R}^n$ and $\mathbf{R}^{n+1/2}$, resampled at each step, are vectors of independent Gaussian white noise with zero mean and unit variance. Note that a useful alternative for SVV is the velocity Verlet implementation of Shardlow's splitting scheme [43, 59], which outperforms SVV in constant energy and constant enthalpy ensembles, while in the cases of constant pressure and temperature that we are considering here, SVV has very comparable performance [33, 42].

Copyright © by SIAM. Unauthorized reproduction of this article is prohibited.

Downloaded 10/30/20 to 59.64.129.2. Redistribution subject to SIAM license or copyright; see https://epubs.siam.org/page/terms

4.3.2. The BAOAB Method. Numerical integration methods, particularly the so-called splitting methods, for Langevin dynamics have been studied systematically in terms of long term sampling performance by Leimkuhler and coworkers [34, 35, 36, 37, 38]. It was demonstrated that, in terms of sampling configurational quantities, a particular choice of splitting method, i.e., the "BAOAB" method, relying on a Trotter factorization of the stochastic vector field of the original (whole) system into exactly solvable subsystems, is far more advantageous than alternative schemes. Subsequently, the optimal design of splitting methods on stochastic dynamics was studied in a variety of applications [39, 40, 41, 58]. We point out that the framework of long-time Talay–Tubaro expansion [1, 2, 12, 34, 35, 36, 37, 40, 60] can be performed trivially in order to analyze the accuracy of ergodic averages (i.e., averages with respect to the invariant measure) in those systems. We separate the vector field of the Langevin dynamics as

$$\mathrm{d}\begin{bmatrix}\mathbf{q}\\ \mathbf{p}\end{bmatrix} = \underbrace{\begin{bmatrix}\mathbf{p}\\ \mathbf{0}\end{bmatrix}\mathrm{d}t}_{\mathrm{A}} + \underbrace{\begin{bmatrix}\mathbf{0}\\ -s\mathbf{q}\end{bmatrix}\mathrm{d}t}_{\mathrm{B}} + \underbrace{\begin{bmatrix}\mathbf{0}\\ -2(\mathbf{p}-\mathbf{u})+\boldsymbol{\eta}\end{bmatrix}}_{\mathrm{O}}, \tag{4.8}$$

where we can solve each piece "exactly." That is, both the "A" and "B" pieces can be straightforwardly solved, while it is also possible to derive the exact solution to the Ornstein–Uhlenbeck ("O") part (see solutions in [58] for more general settings),

$$\mathrm{d}\mathbf{p} = 2\mathbf{u}\mathrm{d}t - 2\mathbf{p}\mathrm{d}t + \boldsymbol{\eta}\,, \tag{4.9}$$

as

$$\mathbf{p}(t) = \mathbf{u} + (\mathbf{p}(0)-\mathbf{u})\,e^{-2t} + \left(\sqrt{1-e^{-4t}}/2\right)\mathbf{R}\,. \tag{4.10}$$

The BAOAB method can then be defined as

$$e^{h\hat{\mathcal{L}}_{\mathrm{BAOAB}}} = e^{(h/2)\mathcal{L}_{\mathrm{B}}}e^{(h/2)\mathcal{L}_{\mathrm{A}}}e^{h\mathcal{L}_{\mathrm{O}}}e^{(h/2)\mathcal{L}_{\mathrm{A}}}e^{(h/2)\mathcal{L}_{\mathrm{B}}}\,, \tag{4.11}$$

where $\exp(h\mathcal{L}_f)$ represents the phase space propagator associated with the corresponding vector field f. More precisely, the integration steps of the BAOAB method, including the streaming velocity, read

$$\mathbf{p}^{n+1/2} = \mathbf{p}^n - hs\mathbf{q}^n/2\,, \tag{4.12a}$$

$$\mathbf{q}^{n+1/2} = \mathbf{q}^n + h\mathbf{p}^{n+1/2}/2\,, \tag{4.12b}$$

$$\tilde{\mathbf{p}}^{n+1/2} = \mathbf{u}^{n+1/2} + \left(\mathbf{p}^{n+1/2}-\mathbf{u}^{n+1/2}\right)e^{-2h} + \left(\sqrt{1-e^{-4h}}/2\right)\mathbf{R}^n\,, \tag{4.12c}$$

$$\mathbf{q}^{n+1} = \mathbf{q}^{n+1/2} + h\tilde{\mathbf{p}}^{n+1/2}/2\,, \tag{4.12d}$$

$$\mathbf{p}^{n+1} = \tilde{\mathbf{p}}^{n+1/2} - hs\mathbf{q}^{n+1}/2\,. \tag{4.12e}$$

Note that only one force calculation is required at each step for the BAOAB method (i.e., the force computed at the end of each step will be reused at the start of the subsequent step), which is the same as for alternative schemes including the SVV method.

5. Numerical Experiments. In this section, we conduct a variety of numerical experiments to compare the performance of the various methods introduced in section 4 in the noninertial (Brownian) and inertial (Langevin) cases, respectively.

Copyright © by SIAM. Unauthorized reproduction of this article is prohibited.

Downloaded 10/30/20 to 59.64.129.2. Redistribution subject to SIAM license or copyright; see https://epubs.siam.org/page/terms

5.1. Simulation Details. As described at the beginning of section 3, we restrict our attention to a single harmonic oscillator of mass m in the presence of a streaming background medium with velocity field $\mathbf{u}$. For the sake of simplicity, we have excluded the diagonal contributions from the matrix $\boldsymbol{\kappa}$ (2.4) in our numerical experiments. In both cases, the parameter set $k = 2$, $k_{\mathrm{B}}T = 0.25$, $\gamma = 2$, $\kappa_{xy} = 1$ was used, resulting in $\omega = k/\gamma = 1$ and $D = k_{\mathrm{B}}T/\gamma = 0.125$ in the Brownian case. The mass was set as unity in the Langevin case, thereby leading to $s = 2$ and $r = 1$. For this choice of parameters, the reference t_{ref} of the Langevin dynamics coincides with the characteristic relaxation time of the inertia-free Brownian case. The initial position of the particle was set at the origin in both cases, while the initial momentum in the Langevin case was zero. Unless otherwise stated, the system was simulated for 1000 reduced time units in both cases, but only the last 80% of the data were collected to calculate the various quantities derived in section 3.

5.2. Results. In order to verify the derivations of the stationary time correlation functions in both the noninertial (subsection 3.2) and the inertial (subsection 3.4) cases, we plot the computed (and normalized) time correlation functions against the analytical solutions in Figures 2 and 3, respectively. It appears that in both cases the numerical solutions are indistinguishable from the analytical solutions with a small stepsize of $h = 0.01$. However, as stepsize increases, the time correlation functions do start deviating from the analytical solutions, which leads to the investigation of the accuracy control of average quantities in subsequent figures. We also want to point out that with the same stepsize $h = 0.01$ but a smaller shear rate, say, $\kappa_{xy} = 0.1$, visible deviations were observed in both cross-correlation functions, i.e., $\langle x(t)y(0)\rangle / \langle xy\rangle$ and $\langle y(t)x(0)\rangle / \langle yx\rangle$, while both autocorrelation functions, i.e., $\langle y(t)y(0)\rangle / \langle y^2\rangle$ and $\langle x(t)x(0)\rangle / \langle x^2\rangle$, were still indistinguishable from the analytical solutions. Moreover, the deviations became even stronger if the shear rate was further reduced. This indicates that both cross-correlation functions are more sensitive to the strength of the shear rate.

The accuracy control of average quantities is often used to measure the performance of the numerical methods. To this end, the computed absolute errors in averages $\langle y^2\rangle$ and $\langle x^2\rangle$ were plotted in Figures 4 and 5 for both the Brownian and the Langevin cases, respectively. (We did not observe significant difference between the methods in both cases in terms of the errors on time correlation functions.) Note that the average $\langle y^2\rangle$ is actually proportional to the so-called configurational temperature (see more discussions in [39, 41]), in this case $k\langle y^2\rangle = k_{\mathrm{B}}T$, which is an important quantity that numerical methods should preserve. The results of $\langle xy\rangle$ were not included due to its sensitivity to sampling errors. To be more specific, in the Brownian case in Figure 4, the limit method is orders of magnitude more accurate than the EM method in $\langle y^2\rangle$, while the former still outperforms the latter in $\langle x^2\rangle$. Although the limit method does not seem to display a second order convergence to the invariant measure as expected in the equilibrium case of $\langle y^2\rangle$, we point out that it might be very challenging to overcome the impact of sampling errors at such a high level of accuracy with the reference value being $\langle y^2\rangle = 0.125$.

In the case of Langevin dynamics, as can be seen in Figure 5, the BAOAB method is also orders of magnitude more accurate than the SVV method in $\langle y^2\rangle$, while the former slightly outperforms the latter in $\langle x^2\rangle$. Interestingly, in the equilibrium case of $\langle y^2\rangle$, the accuracy of the BAOAB method does not seem to depend on the stepsize (although it still seems to fluctuate slightly due to the sampling errors at such a high level of accuracy with the reference value again being $\langle y^2\rangle = 0.125$). This behavior is

Copyright © by SIAM. Unauthorized reproduction of this article is prohibited.

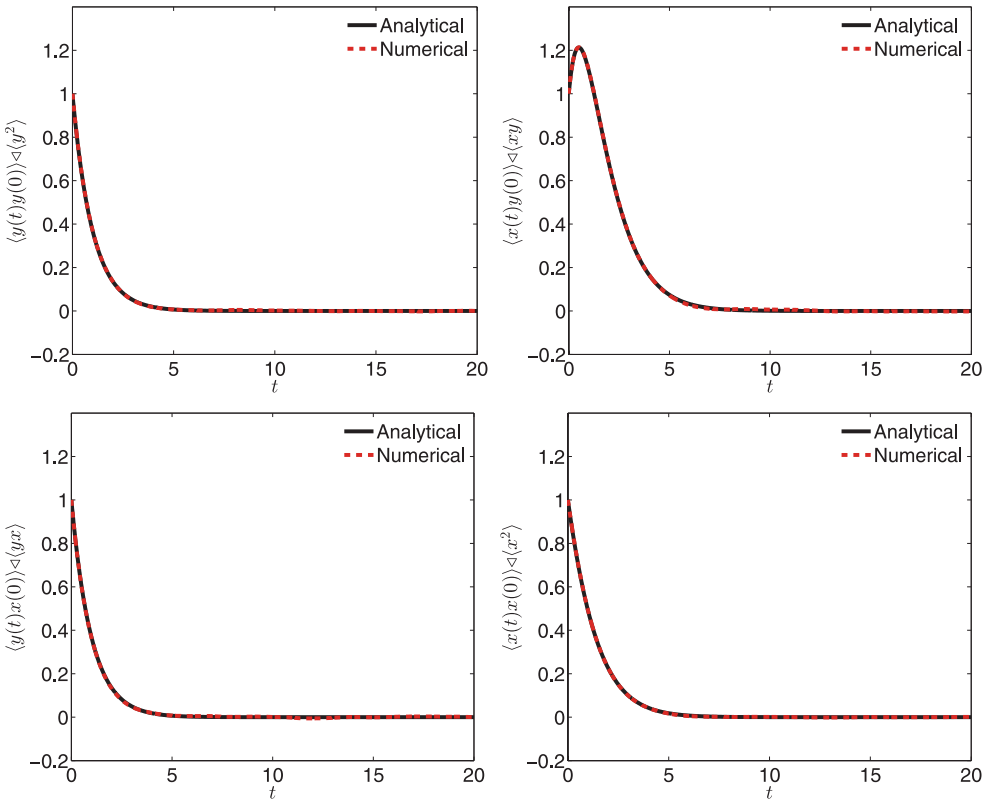

Fig. 2 *Comparison of various computed (and normalized) stationary time correlation functions of Langevin dynamics without inertia (i.e., Brownian dynamics), using the limit method with a stepsize of* $h = 0.01$ *against the analytical solutions derived in subsection* 3.2 *in solid black lines. The system was simulated for* 1000 *reduced time units in each case, but only the last* 80% *of the snapshots were collected to calculate the correlations. Furthermore,* 1000 *different runs were averaged to reduce the sampling errors.*

actually consistent with the demonstration in [35] that the BAOAB method "exactly" preserves the average quantity of $\langle y^2\rangle$ in this particular case.

6. Summary and Outlook. We have derived various time correlation functions and associated quantities of the linear Langevin dynamics (both with and without inertial effects) for a harmonic oscillator in the presence of friction, additive noise, and an external field with both rotational and deformational contributions. We have demonstrated how, in the nontrivial limit of vanishing mass, the inertial results reduce to their noninertial counterparts. While all results were derived explicitly using a straightforward approach suitable for a classroom, we have mentioned two alternative approaches based on (i) the Fourier transform and (ii) the Fokker–Planck equation. In our numerical experiments, for which algorithms were stated in section 4, we have not only verified various time correlation functions (3.30) derived in this article for the benchmark (2.13), but also demonstrated the importance of optimal design of numerical methods. To be more specific, in the Brownian case, we have shown that the limit method substantially outperforms the popular EM method in equilibrium,

Downloaded 10/30/20 to 59.64.129.2. Redistribution subject to SIAM license or copyright; see https://epubs.siam.org/page/terms

Copyright © by SIAM. Unauthorized reproduction of this article is prohibited.

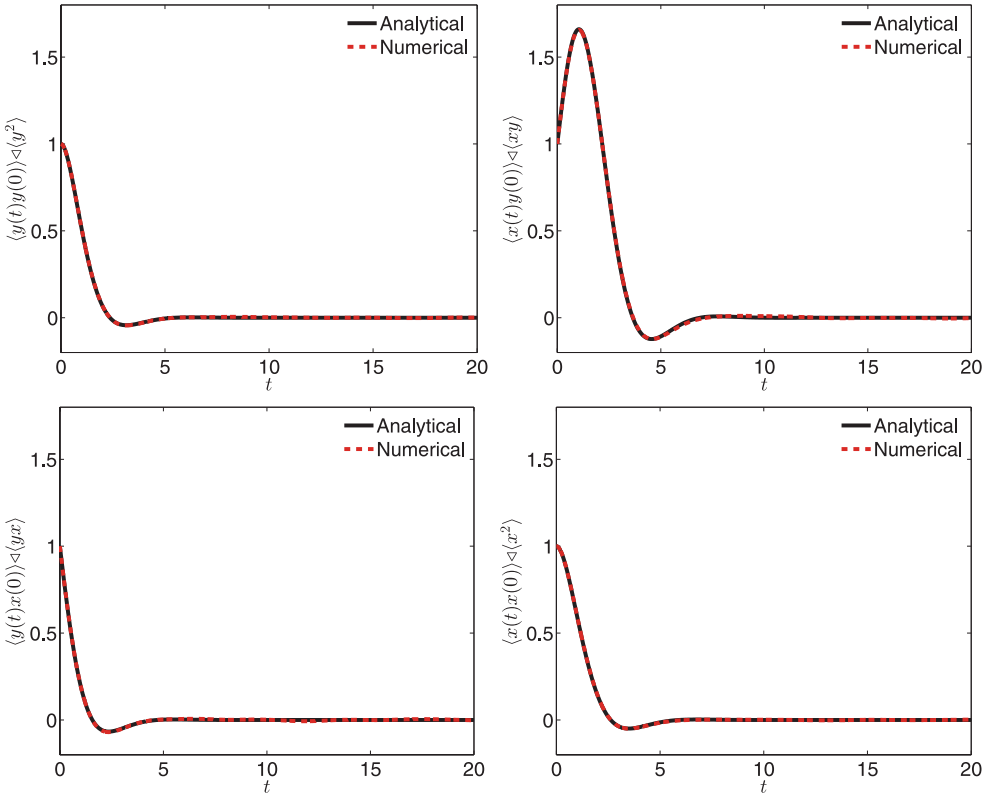

Fig. 3 *Comparison of various computed (and normalized) stationary time correlation functions of Langevin dynamics with inertia using the BAOAB method with stepsize* $h = 0.01$ *against the analytical solutions derived in subsection* 3.4 *in solid black lines. The format of the plots is the same as in Figure* 2.

while the former appears to be still visibly more accurate than the latter in nonequilibrium. On the other hand, in the case of Langevin dynamics, the BAOAB method is orders of magnitude more accurate than the SVV method in equilibrium, whereas the former appears to be only slightly better than the latter in nonequilibrium. While the benchmark (2.13) involves only dimensionless parameters, we have explicitly stated its connection with dimensional equations from real world applications. One of these is the study of the full Rouse model [14, 56] (bead-spring chain, i.e., coupled harmonic oscillators with masses, whose eigenmodes behave as harmonic oscillators) for the short-time and high frequency dynamics of unentangled polymeric systems subject to flows. With the time correlation functions for $\mathbf{q}$ obeying (2.1) at hand, all relevant properties of a bead-spring chain subject to flow can be written down upon replacing m, k, and γ by their mode-dependent counterparts m_p, k_p, and γ_p [14], where $p = 0, 1, 2, \ldots, N$ enumerates the N normal modes of a chain with $N-1$ segments connecting N mass points (beads). In the limit of vanishing mass the known solution of the Rouse model [14] is also recovered this way. The analytical methods applied here to solve the linear Langevin dynamics characterized by matrices $\mathbf{A}$ and $\mathbf{B}$ in (3.53) apply without modification to arbitrary $\mathbf{A}$ and $\mathbf{B}$. The numerical methods apply to both linear and nonlinear problems. These include, for example, the finite extendable

Copyright © by SIAM. Unauthorized reproduction of this article is prohibited.

Downloaded 10/30/20 to 59.64.129.2. Redistribution subject to SIAM license or copyright; see https://epubs.siam.org/page/terms

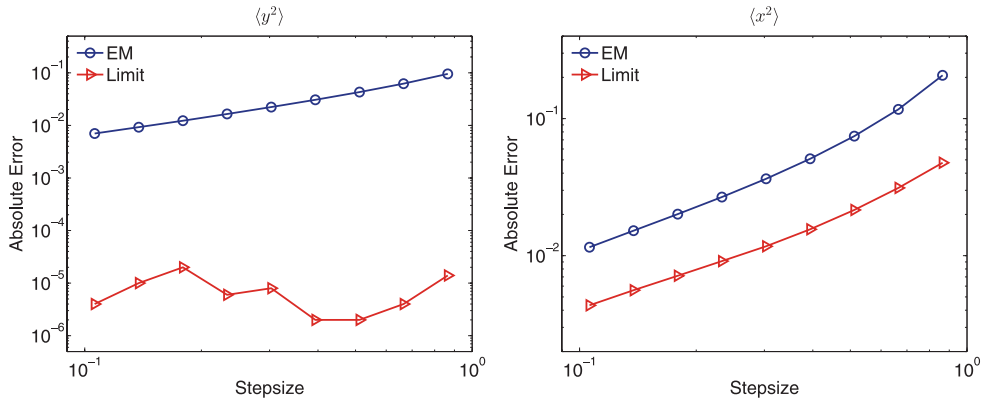

Fig. 4 *Double logarithmic plot of the computed absolute errors in averages* $\langle y^2 \rangle$ *(left) and* $\langle x^2 \rangle$ *(right) derived in subsection* 3.2 *(Brownian dynamics) against stepsize using the EM and limit methods with* $\omega = 1$ *and* $D = 0.125$*. The system was simulated for* 1000 *reduced time units in each case, but only the last* 80% *of the snapshots were collected to calculate the static quantities. Furthermore,* 100,000 *different runs were averaged to reduce the sampling errors. The stepsizes tested began at* $h = 0.106$ *and were increased incrementally by* 30% *until substantial errors in correlations were observed. Error bars for the EM and limit methods are comparable to symbol sizes and thus not presented.*

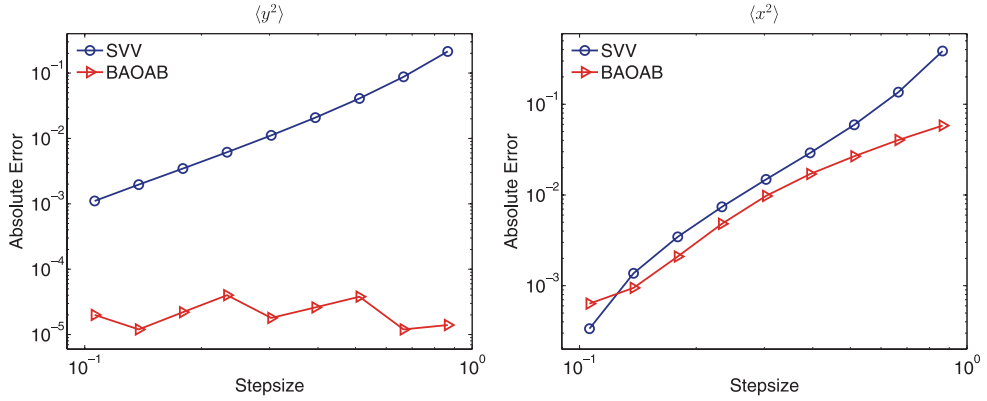

Fig. 5 *Double logarithmic plot of the computed absolute errors in averages* $\langle y^2 \rangle$ *(left) and* $\langle x^2 \rangle$ *(right) derived in subsection* 3.4 *(Langevin dynamics) against stepsize using the SVV and BAOAB methods with* $s = 2$ *and* $r = 1$*. The format of the plots is the same as in Figure* 4*. Error bars for the SVV and BAOAB methods are comparable to symbol sizes and thus not presented.*

nonlinear elastic (FENE) dumbbell or multibead chain models [21, 25, 30]. Their approximate analytical treatment remains beyond the scope of this contribution; for a numerical implementation, see, e.g., [54].

Appendix A. Nondimensionalization. In what follows we show that the nondimensionalized version of (2.5) is (2.13). Dimensionless quantities f_* are introduced via $f = f_* f_{\mathrm{ref}}$, in general, with reference quantities f_{ref} carrying the physical dimension. Having restored the asterisks dropped and also having rewritten the noise term as a derivative (although it is not rigorously defined in the usual mathematical

Copyright © by SIAM. Unauthorized reproduction of this article is prohibited.

Downloaded 10/30/20 to 59.64.129.2. Redistribution subject to SIAM license or copyright; see https://epubs.siam.org/page/terms

Downloaded 10/30/20 to 59.64.129.2. Redistribution subject to SIAM license or copyright; see https://epubs.siam.org/page/terms

sense), (2.13a) reads

$$\frac{\mathrm{d}^2 x_*}{\mathrm{d}t_*^2} = -s_x x_* - 2\left(\frac{\mathrm{d}x_*}{\mathrm{d}t_*} - r y_*\right) + \frac{\mathrm{dW}_{*,x}}{\mathrm{d}t_*}\,. \tag{A.1}$$

Since W^2 has the dimension of time, $\mathrm{W}_{\mathrm{ref}} = \sqrt{t_{\mathrm{ref}}}$, and (A.1), upon replacing f_* by f/f_{ref} and subsequent multiplication by $mq_{\mathrm{ref}}/t_{\mathrm{ref}}^2$ on both sides of the equation, becomes

$$m\frac{\mathrm{d}^2 x}{\mathrm{d}t^2} = -s_x \frac{mx}{t_{\mathrm{ref}}^2} - 2\left(\frac{m}{t_{\mathrm{ref}}}\frac{\mathrm{d}x}{\mathrm{d}t} - r\frac{my}{t_{\mathrm{ref}}^2}\right) + mq_{\mathrm{ref}}\frac{t_{\mathrm{ref}}^{1/2}}{t_{\mathrm{ref}}^2}\frac{\mathrm{dW}_x}{\mathrm{d}t}\,. \tag{A.2}$$

Proof. Inserting q_{ref}, t_{ref}, s_μ, and r from (2.11) and (2.12) into (A.2),

$$\begin{aligned} m\frac{\mathrm{d}^2 x}{\mathrm{d}t^2} &= -\frac{4mk_x}{\gamma^2}\frac{m\gamma^2 x}{4m^2} - 2\left(\frac{m\gamma}{2m}\frac{\mathrm{d}x}{\mathrm{d}t} - \frac{2m\kappa_{xy}}{\gamma}\frac{m\gamma^2 y}{4m^2}\right) + m\frac{2^{3/2}\sigma\sqrt{m}}{\gamma^{3/2}}\left(\frac{\gamma}{2m}\right)^{3/2}\frac{\mathrm{dW}_x}{\mathrm{d}t} \\ &= -k_x x - \gamma\left(\frac{\mathrm{d}x}{\mathrm{d}t} - \kappa_{xy} y\right) + \sigma\frac{\mathrm{dW}_x}{\mathrm{d}t}\,. \end{aligned} \tag{A.3}$$

∎

Appendix B. Ideal Brownian Dynamics: $m = 0, k_x = k_y = 0$.

B.1. Time Correlation Function $\langle[x(t) - x(0)][y(t) - y(0)]\rangle$.

Proof. Starting from (3.1), with the help of (2.3), we arrive at (3.5) as follows:

$$\begin{aligned} \langle[x(t)-x(0)][y(t)-y(0)]\rangle &= \left\langle \int_0^t \dot{x}(t_1)\,\mathrm{d}t_1 \int_0^t \dot{y}(t_2)\,\mathrm{d}t_2 \right\rangle \\ &= \sqrt{2D}\int_0^t\int_0^t \left[\kappa_{xy}\,\langle y(t_1)\eta_y(t_2)\rangle + \sqrt{2D}\,\langle \eta_x(t_1)\,\eta_y(t_2)\rangle\right]\mathrm{d}t_2\mathrm{d}t_1 \\ &= 2D\kappa_{xy}\int_0^t\int_0^t\int_0^{t_1} \langle \eta_y(t_1')\eta_y(t_2)\rangle\,\mathrm{d}t_1'\,\mathrm{d}t_2\,\mathrm{d}t_1 \\ &= 2D\kappa_{xy}\int_0^t\int_0^t\int_0^{t_1} \delta(t_1'-t_2)\,\mathrm{d}t_1'\,\mathrm{d}t_2\,\mathrm{d}t_1 \\ &= 2D\kappa_{xy}\int_0^t\int_0^{t_1}\int_0^{t_1} \delta(t_1'-t_2)\,\mathrm{d}t_1'\,\mathrm{d}t_2\,\mathrm{d}t_1 \\ &= 2D\kappa_{xy}\int_0^t\int_0^{t_1} \mathrm{d}t_2\,\mathrm{d}t_1 = D\kappa_{xy}t^2\,. \end{aligned} \tag{B.1}$$

∎

Copyright © by SIAM. Unauthorized reproduction of this article is prohibited.

Downloaded 10/30/20 to 59.64.129.2. Redistribution subject to SIAM license or copyright; see https://epubs.siam.org/page/terms

B.2. Mean Squared Displacement $\langle [x(t) - x(0)]^2 \rangle$.

Proof. Starting from (3.1), with the help of (2.3), we arrive at (3.6) as follows:

$$\begin{aligned}
\left\langle [x(t) - x(0)]^2 \right\rangle &= \left\langle \int_0^t \dot{x}(t_1)\,\mathrm{d}t_1 \int_0^t \dot{x}(t_2)\,\mathrm{d}t_2 \right\rangle \\
&= \int_0^t \int_0^t \left[2D\,\delta(t_1 - t_2) + \kappa_{xy}^2 \langle y(t_1) y(t_2) \rangle \right] \mathrm{d}t_1\,\mathrm{d}t_2 \\
&= 2Dt + \kappa_{xy}^2 \int_0^t \int_0^t \left[2D \min(t_1, t_2) + y_0^2 \right] \mathrm{d}t_1\,\mathrm{d}t_2 \\
&= 2Dt + 2D\kappa_{xy}^2 \left(\int_0^t \int_{t_2}^t t_2 \mathrm{d}t_1 \mathrm{d}t_2 + \int_0^t \int_0^{t_2} t_1 \mathrm{d}t_1 \mathrm{d}t_2 \right) + (\kappa_{xy} y_0 t)^2 \\
&= 2Dt \left[1 + \frac{1}{3} (\kappa_{xy} t)^2 \right] + (\kappa_{xy} y_0 t)^2 \,. \qquad \text{(B.2)}
\end{aligned}$$

∎

Appendix C. Nonideal Brownian Dynamics: $m = 0, k_x, k_y > 0$.

C.1. Time Correlation Function $\langle y(t_1) y(t_2) \rangle$.

Proof. Starting from (3.7b), with the help of (2.3) together with the identity $\min(t_1, t_2) = (t_1 + t_2)/2 - |t_1 - t_2|/2$, (3.8) is obtained as follows:

$$\begin{aligned}
\langle y(t_1) y(t_2) \rangle &= 2D \left\langle \int_{-\infty}^{t_1} \eta_y(t_1') e^{-\omega_y (t_1 - t_1')}\,\mathrm{d}t_1' \int_{-\infty}^{t_2} \eta_y(t_2') e^{-\omega_y (t_2 - t_2')}\,\mathrm{d}t_2' \right\rangle \\
&= 2D \int_{-\infty}^{t_1} \int_{-\infty}^{t_2} e^{-\omega_y (t_1 + t_2 - t_1' - t_2')} \langle \eta_y(t_1')\, \eta_y(t_2') \rangle\,\mathrm{d}t_2'\,\mathrm{d}t_1' \\
&= 2D \int_{-\infty}^{t_1} \int_{-\infty}^{t_2} e^{-\omega_y (t_1 + t_2 - t_1' - t_2')}\, \delta(t_1' - t_2')\,\mathrm{d}t_2'\,\mathrm{d}t_1' \\
&= 2D \int_{-\infty}^{\min(t_1, t_2)} e^{-\omega_y (t_1 + t_2 - 2t_1')}\,\mathrm{d}t_1' \\
&= \frac{D}{\omega_y} e^{-\omega_y |t_1 - t_2|} \,. \qquad \text{(C.1)}
\end{aligned}$$

∎

C.2. Time Correlation Function $\langle x(t) y(0) \rangle$.

Proof. Starting from (3.7b), an intermediate result is

$$\begin{aligned}
\langle y(t_1)\, \eta_y(t_2) \rangle &= \sqrt{2D} \int_{-\infty}^{t_1} \langle \eta_y(t_1')\, \eta_y(t_2) \rangle\, e^{-\omega_y (t_1 - t_1')}\,\mathrm{d}t_1' \\
&= \sqrt{2D} \int_{-\infty}^{t_1} \delta(t_1' - t_2) e^{-\omega_y (t_1 - t_1')}\,\mathrm{d}t_1' \\
&= \sqrt{2D}\, e^{-\omega_y (t_1 - t_2)} \Theta(t_1 - t_2) \,, \qquad \text{(C.2)}
\end{aligned}$$

where Θ denotes the Heaviside step function. Since $\langle \eta_x(t)\, \eta_y(t') \rangle = 0$, one recov-

Copyright © by SIAM. Unauthorized reproduction of this article is prohibited.

Downloaded 10/30/20 to 59.64.129.2. Redistribution subject to SIAM license or copyright; see https://epubs.siam.org/page/terms

ers (3.10a) using (C.2),

$$\begin{aligned}\langle x(t)y(0)\rangle &= \sqrt{2D}\int_{-\infty}^{t}\int_{-\infty}^{0}\left\langle\left[\kappa_{xy}y(t_1)+\sqrt{2D}\,\eta_x(t_1)\right]\eta_y(t_2)\right\rangle e^{-\omega_x(t-t_1)+\omega_y t_2}\,\mathrm{d}t_2\,\mathrm{d}t_1\\ &= 2D\kappa_{xy}\int_{-\infty}^{t}\int_{-\infty}^{0} e^{-\omega_y(t_1-t_2)}\Theta(t_1-t_2)e^{-\omega_x(t-t_1)+\omega_y t_2}\,\mathrm{d}t_2\,\mathrm{d}t_1\\ &= 2D\kappa_{xy}e^{-\omega_x t}\int_{-\infty}^{0} e^{2\omega_y t_2}\int_{t_2}^{t} e^{(\omega_x-\omega_y)t_1}\,\mathrm{d}t_1\,\mathrm{d}t_2\\ &= D\kappa_{xy}\,\frac{(\omega_x+\omega_y)e^{-\omega_y t}-2\omega_y e^{-\omega_x t}}{(\omega_x^2-\omega_y^2)\omega_y}\,. \qquad \text{(C.3)}\end{aligned}$$

∎

C.3. Time Correlation Function $\langle y(t)x(0)\rangle$.

Proof. In full analogy to Appendix C.2, (3.10b) is derived via

$$\begin{aligned}\langle y(t)x(0)\rangle &= \sqrt{2D}\int_{-\infty}^{t}\int_{-\infty}^{0}\left\langle\eta_y(t_1)\left[\kappa_{xy}y(t_2)+\sqrt{2D}\,\eta_x(t_2)\right]\right\rangle e^{-\omega_y(t-t_1)+\omega_x t_2}\,\mathrm{d}t_2\,\mathrm{d}t_1\\ &= 2D\kappa_{xy}\int_{-\infty}^{t}\int_{-\infty}^{0} e^{-\omega_y(t_2-t_1)}\Theta(t_2-t_1)e^{-\omega_y(t-t_1)+\omega_x t_2}\,\mathrm{d}t_2\,\mathrm{d}t_1\\ &= 2D\kappa_{xy}e^{-\omega_y t}\int_{-\infty}^{0} e^{(\omega_x-\omega_y)t_2}\int_{-\infty}^{t_2} e^{2\omega_y t_1}\,\mathrm{d}t_1\,\mathrm{d}t_2\\ &= \frac{D\kappa_{xy}e^{-\omega_y t}}{(\omega_x+\omega_y)\omega_y}\,. \qquad \text{(C.4)}\end{aligned}$$

∎

C.4. Time Correlation Function $\langle x(t)x(0)\rangle$.

Proof. The solution (3.7a) can be written as the sum of two uncorrelated contributions $x(t)=x_1(t)+x_2(t)$, where $x_1(t)$ and $x_2(t)$ are given by

$$x_1(t)=\kappa_{xy}\int_{-\infty}^{t} y(t')e^{-\omega_x(t-t')}\,\mathrm{d}t'\,,\quad x_2(t)=\sqrt{2D}\int_{-\infty}^{t}\eta_x(t')e^{-\omega_x(t-t')}\,\mathrm{d}t'\,. \qquad \text{(C.5)}$$

While $\langle x_2(t)x_2(0)\rangle$ can be immediately obtained from (3.7b) and (3.9) as

$$\langle x_2(t)x_2(0)\rangle = \frac{De^{-\omega_x t}}{\omega_x}\,, \qquad \text{(C.6)}$$

and since the cross-correlation $\langle x_1(t)x_2(0)\rangle$ vanishes for all t as $\langle\eta_x(t)\eta_y(0)\rangle$ does, the remaining contribution to $\langle x(t)x(0)\rangle$ is

$$\begin{aligned}\langle x_1(t)x_1(0)\rangle &= \kappa_{xy}^2\int_{-\infty}^{t}\int_{-\infty}^{0}\langle y(t_1)y(t_2)\rangle\, e^{-\omega_x(t-t_1-t_2)}\,\mathrm{d}t_2\,\mathrm{d}t_1\\ &= \frac{\kappa_{xy}^2 D}{\omega_y}\int_{-\infty}^{t}\int_{-\infty}^{0} e^{-\omega_y|t_1-t_2|}e^{-\omega_x(t-t_1-t_2)}\,\mathrm{d}t_2\,\mathrm{d}t_1\\ &= \frac{\kappa_{xy}^2 De^{-\omega_x t}}{\omega_y}\left[\int_{-\infty}^{0} e^{(\omega_x+\omega_y)t_2}\int_{t_2}^{t} e^{(\omega_x-\omega_y)t_1}\,\mathrm{d}t_1\,\mathrm{d}t_2\right.\\ &\qquad\left.+\int_{-\infty}^{0} e^{(\omega_x-\omega_y)t_2}\int_{-\infty}^{t_2} e^{(\omega_x+\omega_y)t_1}\,\mathrm{d}t_1\,\mathrm{d}t_2\right]\\ &= \frac{\kappa_{xy}^2 D\left(\omega_x e^{-\omega_y t}-\omega_y e^{-\omega_x t}\right)}{(\omega_x^2-\omega_y^2)\omega_x\omega_y}\,. \qquad \text{(C.7)}\end{aligned}$$

The sum of (C.6) and (C.7) is the desired expression (3.12) for $\langle x(t)x(0)\rangle$. ∎

Copyright © by SIAM. Unauthorized reproduction of this article is prohibited.

Downloaded 10/30/20 to 59.64.129.2. Redistribution subject to SIAM license or copyright; see https://epubs.siam.org/page/terms

Appendix D. Ideal Langevin Dynamics: $m > 0, k_x = k_y = 0$.

D.1. Mean Squared Displacement $\langle [y(t) - y(0)]^2 \rangle$.

Proof. Rewriting $y(t) - y(0)$ as an integral, using (3.18b), we arrive at (3.20) as follows:

$$\begin{aligned}\left\langle [y(t) - y(0)]^2 \right\rangle &= \left\langle \int_0^t \dot{y}(t_1)\,\mathrm{d}t_1 \int_0^t \dot{y}(t_2)\,\mathrm{d}t_2 \right\rangle \\ &= \int_0^t \int_0^t \langle \dot{y}(t_1)\dot{y}(t_2)\rangle \,\mathrm{d}t_1\,\mathrm{d}t_2 = \frac{1}{4}\int_0^t \int_0^t e^{-2|t_1-t_2|}\,\mathrm{d}t_1\,\mathrm{d}t_2 \\ &= \frac{1}{4}\left[\int_0^t e^{-2t_1}\int_0^{t_1} e^{2t_2}\,\mathrm{d}t_2\,\mathrm{d}t_1 + \int_0^t e^{2t_1}\int_{t_1}^t e^{-2t_2}\,\mathrm{d}t_2\,\mathrm{d}t_1\right] \\ &= \frac{1}{8}\left(2t + e^{-2t} - 1\right). \qquad \text{(D.1)}\end{aligned}$$

∎

Appendix E. Nonideal Langevin Dynamics: $m > 0, k \equiv k_x = k_y > 0$.

E.1. Solution of the System $y(t)$.

Proof. Let

$$G_y^{\pm}(t) = G_y(t, s_\pm) = e^{-s_\pm t}\int_{-\infty}^t e^{s_\pm t'}\eta_y(t')\,\mathrm{d}t'. \qquad \text{(E.1)}$$

Equation (3.25) may be rewritten as

$$2\sqrt{1-s}\,y = G_y^- - G_y^+. \qquad \text{(E.2)}$$

Differentiating this expression with respect t gives

$$2\sqrt{1-s}\,\dot{y} = -s_- G_y^- + s_+ G_y^+, \qquad \text{(E.3)}$$

and differentiating once more with respect to t gives

$$2\sqrt{1-s}\,\ddot{y} = s_-^2 G_y^- - s_+^2 G_y^+ + (s_+ - s_-)\eta_y. \qquad \text{(E.4)}$$

Substituting the above three equations into (3.24b), we have proven (3.25). ∎

E.2. Time Correlation Function $\langle y(t)y(0)\rangle$.

Proof. We begin with the intermediate result

$$\begin{aligned}\langle G_y(t,a)G_y(0,b)\rangle &= \left\langle \int_{-\infty}^t e^{-a(t-t_1)}\,\eta_y(t_1)\,\mathrm{d}t_1 \int_{-\infty}^0 e^{-b(0-t_2)}\,\eta_y(t_2)\,\mathrm{d}t_2 \right\rangle \\ &= \int_{-\infty}^t \int_{-\infty}^0 e^{-a(t-t_1)+bt_2}\,\langle \eta_y(t_1)\,\eta_y(t_2)\rangle\,\mathrm{d}t_2\,\mathrm{d}t_1 \\ &= \int_{-\infty}^t \int_{-\infty}^0 e^{-a(t-t_1)+bt_2}\,\delta(t_1-t_2)\,\mathrm{d}t_2\,\mathrm{d}t_1 \\ &= e^{-at}\int_{-\infty}^0 e^{(a+b)t_1}\,\mathrm{d}t_1 \\ &= \frac{e^{-at}}{a+b} \qquad [\Re(a+b) > 0]. \qquad \text{(E.5)}\end{aligned}$$

Copyright © by SIAM. Unauthorized reproduction of this article is prohibited.

Downloaded 10/30/20 to 59.64.129.2. Redistribution subject to SIAM license or copyright; see https://epubs.siam.org/page/terms

Given $a, b \in \{s_-, s_+\}$, one can verify that the real parts of $a + b$ are always positive. Therefore, starting from (3.25) one approves (3.30a) with the help of (E.5):

$$\begin{aligned}\langle y(t)y(0)\rangle &= \frac{1}{4(1-s)}\left\langle [G_y(t,s_-) - G_y(t,s_+)]\,[G_y(0,s_-) - G_y(0,s_+)]\right\rangle \\ &= \frac{1}{4(1-s)}\left[\frac{e^{-s_-t}}{2s_-} - \frac{e^{-s_-t}}{s_- + s_+} - \frac{e^{-s_+t}}{s_- + s_+} + \frac{e^{-s_+t}}{2s_+}\right] \\ &= \frac{1}{8s\sqrt{1-s}}(C_1^+ + C_1^-)\,. \qquad \text{(E.6)}\end{aligned}$$

∎

E.3. Time Correlation Function $\langle x(t)y(0)\rangle$.

Proof. We need the intermediate results

$$\begin{aligned}\langle G_y(t_1,s')\,\eta_y(t_2)\rangle &= \left\langle \int_{-\infty}^{t_1} e^{-s'(t_1-t')}\,\eta_y(t')\,\eta_y(t_2)\,\mathrm{d}t' \right\rangle \\ &= \int_{-\infty}^{t_1} e^{-s'(t_1-t')}\,\langle \eta_y(t')\,\eta_y(t_2)\rangle\,\mathrm{d}t' \\ &= \int_{-\infty}^{t_1} e^{-s'(t_1-t')}\,\delta(t'-t_2)\,\mathrm{d}t' \\ &= e^{-s'(t_1-t_2)}\Theta(t_1-t_2) \qquad \text{(E.7)}\end{aligned}$$

and, with $y(t)$ from (3.25),

$$\begin{aligned}\langle y(t_1)\,\eta_y(t_2)\rangle &= \frac{1}{2\sqrt{1-s}}\left\langle [G_y(t_1,s_-) - G_y(t_1,s_+)]\,\eta_y(t_2)\right\rangle \\ &= \frac{1}{2\sqrt{1-s}}\left[\langle G_y(t_1,s_-)\,\eta_y(t_2)\rangle - \langle G_y(t_1,s_+)\,\eta_y(t_2)\rangle\right] \\ &= \frac{1}{2\sqrt{1-s}}\left[e^{-s_-(t_1-t_2)} - e^{-s_+(t_1-t_2)}\right]\Theta(t_1-t_2)\,. \qquad \text{(E.8)}\end{aligned}$$

Using (E.7) and (E.8), with as yet unspecified a and b,

$$\begin{aligned}\left\langle G_x(t,a)G_y(0,b)\right\rangle &= \left\langle \int_{-\infty}^{t} e^{-a(t-t_1)}\,[2ry(t_1) + \eta_x(t_1)]\,\mathrm{d}t_1 \int_{-\infty}^{0} e^{-b(0-t_2)}\,\eta_y(t_2)\,\mathrm{d}t_2 \right\rangle \\ &= 2r\int_{-\infty}^{t}\int_{-\infty}^{0} e^{-a(t-t_1)+bt_2}\,\langle y(t_1)\,\eta_y(t_2)\rangle\,\mathrm{d}t_2\,\mathrm{d}t_1 \\ &= \frac{r}{\sqrt{1-s}}\int_{-\infty}^{t}\int_{-\infty}^{0} e^{-a(t-t_1)+bt_2}\left[e^{-s_-(t_1-t_2)} - e^{-s_+(t_1-t_2)}\right]\Theta(t_1-t_2)\mathrm{d}t_2\mathrm{d}t_1 \\ &= \frac{re^{-at}}{\sqrt{1-s}}\int_{t_2}^{t}\int_{-\infty}^{0} e^{at_1+bt_2}\left[e^{-s_-(t_1-t_2)} - e^{-s_+(t_1-t_2)}\right]\mathrm{d}t_2\,\mathrm{d}t_1\,. \qquad \text{(E.9)}\end{aligned}$$

For all the relevant choices of a and b in (E.9), the integrals can be performed as

Copyright © by SIAM. Unauthorized reproduction of this article is prohibited.

Downloaded 10/30/20 to 59.64.129.2. Redistribution subject to SIAM license or copyright; see https://epubs.siam.org/page/terms

follows:

$$\langle G_x(t,s_-)G_y(0,s_-)\rangle = \frac{re^{-s_-t}}{\sqrt{1-s}}\left[\frac{t}{2s_-}+\frac{1}{4s_-^2}-\frac{1}{s_--s_+}\left(\frac{e^{(s_--s_+)t}}{s_-+s_+}-\frac{1}{2s_-}\right)\right],$$
$$\langle G_x(t,s_-)G_y(0,s_+)\rangle = \frac{re^{-s_-t}}{\sqrt{1-s}}\left[\frac{t}{s_-+s_+}+\frac{1}{(s_-+s_+)^2}-\frac{1}{s_--s_+}\left(\frac{e^{(s_--s_+)t}}{2s_+}-\frac{1}{s_-+s_+}\right)\right],$$
$$\langle G_x(t,s_+)G_y(0,s_-)\rangle = \frac{re^{-s_+t}}{\sqrt{1-s}}\left[\frac{1}{s_+-s_-}\left(\frac{e^{(s_+-s_-)t}}{2s_-}-\frac{1}{s_-+s_+}\right)-\frac{t}{s_-+s_+}-\frac{1}{(s_-+s_+)^2}\right],$$
$$\langle G_x(t,s_+)G_y(0,s_+)\rangle = \frac{re^{-s_+t}}{\sqrt{1-s}}\left[\frac{1}{s_+-s_-}\left(\frac{e^{(s_+-s_-)t}}{s_-+s_+}-\frac{1}{2s_+}\right)-\frac{t}{2s_+}-\frac{1}{4s_+^2}\right].$$

With their help the correlation $\langle x(t)y(0)\rangle$ can now be calculated quite conveniently as

$$\begin{aligned}\langle x(t)y(0)\rangle &= \frac{1}{4(1-s)}\left\langle\left[G_x(t,s_-)-G_x(t,s_+)\right]\left[G_y(0,s_-)-G_y(0,s_+)\right]\right\rangle\\ &= \frac{re^{-s_+t}}{8(1-s)^{3/2}}\frac{\sqrt{1-s}}{\left(1+\sqrt{1-s}\right)}\left[t+\frac{1}{2}\left(1+\frac{1}{1+\sqrt{1-s}}\right)+\frac{1}{\sqrt{1-s}}\right]\\ &\quad -\frac{re^{-s_-t}}{8(1-s)^{3/2}}\frac{\sqrt{1-s}}{\left(1-\sqrt{1-s}\right)}\left[-t-\frac{1}{2}\left(1+\frac{1}{1-\sqrt{1-s}}\right)+\frac{1}{\sqrt{1-s}}\right].\end{aligned}\tag{E.10}$$

Multiplying $\left(1-\sqrt{1-s}\right)^2\left(1+\sqrt{1-s}\right)^2 = s^2$ on both sides gives

$$\begin{aligned}s^2\langle x(t)y(0)\rangle &= \frac{re^{-s_+t}}{8(1-s)^{3/2}}\left(1-\sqrt{1-s}\right)^2\left[(2+t)\sqrt{1-s}+\left(\frac{1}{2}+t\right)(1-s)+1\right]\\ &\quad -\frac{re^{-s_-t}}{8(1-s)^{3/2}}\left(1+\sqrt{1-s}\right)^2\left[-(2+t)\sqrt{1-s}+\left(\frac{1}{2}+t\right)(1-s)+1\right],\end{aligned}\tag{E.11}$$

so that we finally arrive at (3.30a),

$$\langle x(t)y(0)\rangle = \frac{r\left(A^+-A^-\right)}{8s^2(1-s)^{3/2}} = \langle y(-t)x(0)\rangle\,.\tag{E.12}$$

∎

E.4. Time Correlation Function $\langle y(t)x(0)\rangle$.

Proof. Here we need another intermediate result,

$$\begin{aligned}\langle\eta_y(t_1)G_y(t_2,s')\rangle &= \left\langle\int_{-\infty}^{t_2}e^{-s'(t_2-t')}\,\eta_y(t_1)\,\eta_y(t')\,\mathrm{d}t'\right\rangle\\ &= \int_{-\infty}^{t_2}e^{-s'(t_2-t')}\,\langle\eta_y(t_1)\,\eta_y(t')\rangle\,\mathrm{d}t'\\ &= \int_{-\infty}^{t_2}e^{-s'(t_2-t')}\,\delta(t_1-t')\,\mathrm{d}t'\\ &= e^{-s(t_2-t_1)}\Theta(t_2-t_1)\,,\end{aligned}\tag{E.13}$$

Copyright © by SIAM. Unauthorized reproduction of this article is prohibited.

Downloaded 10/30/20 to 59.64.129.2. Redistribution subject to SIAM license or copyright; see https://epubs.siam.org/page/terms

as well as, with $y(t)$ from (3.25),

$$\begin{aligned}\langle \eta_y(t_1) y(t_2)\rangle &= \frac{1}{2\sqrt{1-s}} \langle \eta_y(t_1) \left[G_y(t_2, s_-) - G_y(t_2, s_+)\right]\rangle \\ &= \frac{1}{2\sqrt{1-s}} \left[\langle \eta_y(t_1) G_y(t_2, s_-)\rangle - \langle \eta_y(t_1) G_y(t_2, s_+)\rangle\right] \\ &= \frac{1}{2\sqrt{1-s}} \left[e^{-s_-(t_2-t_1)} - e^{-s_+(t_2-t_1)}\right] \Theta(t_2 - t_1)\,. \end{aligned} \tag{E.14}$$

Making use of (E.13) and (E.14), one has

$$\begin{aligned}\langle G_y(t,a) G_x(0,b)\rangle &= \left\langle \int_{-\infty}^{t} e^{-a(t-t_1)}\, \eta_y(t_1)\, \mathrm{d}t_1 \int_{-\infty}^{0} e^{-b(0-t_2)} \left[2r y(t_2) + \eta_x(t_2)\right] \mathrm{d}t_2 \right\rangle \\ &= 2r \int_{-\infty}^{t}\int_{-\infty}^{0} e^{-a(t-t_1)+bt_2} \langle \eta_y(t_1) y(t_2)\rangle \,\mathrm{d}t_2\,\mathrm{d}t_1 \\ &= \frac{r}{\sqrt{1-s}} \int_{-\infty}^{t}\int_{-\infty}^{0} e^{-a(t-t_1)+bt_2} \left[e^{-s_-(t_2-t_1)} - e^{-s_+(t_2-t_1)}\right] \Theta(t_2-t_1) \mathrm{d}t_2 \mathrm{d}t_1 \\ &= \frac{r e^{-at}}{\sqrt{1-s}} \int_{-\infty}^{t_2}\int_{-\infty}^{0} e^{at_1+bt_2} \left[e^{-s_-(t_2-t_1)} - e^{-s_+(t_2-t_1)}\right] \mathrm{d}t_2\,\mathrm{d}t_1 \\ &= \frac{r e^{-at}}{\sqrt{1-s}} \left[\frac{1}{a+b}\left(\frac{1}{a+s_-} - \frac{1}{a+s_+}\right)\right]. \end{aligned} \tag{E.15}$$

Starting from (3.25) and (3.28), we can then immediately write down

$$\begin{aligned}\langle y(t) x(0)\rangle &= \frac{1}{4(1-s)} \langle \left[G_y(t, s_-) - G_y(t, s_+)\right] \left[G_x(0, s_-) - G_x(0, s_+)\right]\rangle \\ &= \frac{r e^{-s_- t}}{16\sqrt{1-s}} \left(\frac{1}{s_-}\right)^2 - \frac{r e^{-s_+ t}}{16\sqrt{1-s}} \left(\frac{1}{s_+}\right)^2 . \end{aligned} \tag{E.16}$$

Multiplying $\left(1-\sqrt{1-s}\right)^2 \left(1+\sqrt{1-s}\right)^2 = s^2$ on both sides gives

$$s^2 \langle y(t) x(0)\rangle = \frac{r e^{-s_- t}}{16\sqrt{1-s}} \left(1+\sqrt{1-s}\right)^2 - \frac{r e^{-s_+ t}}{16\sqrt{1-s}} \left(1-\sqrt{1-s}\right)^2 , \tag{E.17}$$

so that we have proven (3.30c),

$$\langle y(t) x(0)\rangle = \frac{r\left(C_2^- - C_2^+\right)}{16 s^2 \sqrt{1-s}} = \langle x(-t) y(0)\rangle\,. \tag{E.18}$$

∎

Copyright © by SIAM. Unauthorized reproduction of this article is prohibited.

Downloaded 10/30/20 to 59.64.129.2. Redistribution subject to SIAM license or copyright; see https://epubs.siam.org/page/terms

E.5. Time Correlation Function $\langle x(t)x(0)\rangle$.

Proof. For the sake of completeness and readers' convenience we provide here the full proof of (3.30d). We begin, as before, with an intermediate result,

$$\begin{aligned}
\langle G_y(t_1,a)G_y(t_2,b)\rangle &= \left\langle \int_{-\infty}^{t_1} e^{-a(t_1-t_1')}\,\eta_y(t_1')\,\mathrm{d}t_1' \int_{-\infty}^{t_2} e^{-b(t_2-t_2')}\,\eta_y(t_2')\,\mathrm{d}t_2' \right\rangle \\
&= \int_{-\infty}^{t_1}\int_{-\infty}^{t_2} e^{-a(t_1-t_1')-b(t_2-t_2')}\,\mathrm{d}t_2'\,\mathrm{d}t_1'\,\langle \eta_y(t_1')\,\eta_y(t_2')\rangle \\
&= \int_{-\infty}^{t_1}\int_{-\infty}^{t_2} e^{-a(t_1-t_1')-b(t_2-t_2')}\,\delta(t_1'-t_2')\,\mathrm{d}t_2'\,\mathrm{d}t_1' \\
&= e^{-(at_1+bt_2)}\int_{-\infty}^{\min(t_1,t_2)} e^{(a+b)t_1'}\,\mathrm{d}t_1' \\
&= e^{-(at_1+bt_2)}\frac{e^{(a+b)\min(t_1,t_2)}}{a+b} \qquad [\Re(a+b)>0]\,, \qquad \text{(E.19)}
\end{aligned}$$

which corresponds, for $t_1 \geq t_2$ or $t_1 \leq t_2$, to either

$$\langle G_y(t_1,a)G_y(t_2,b)\rangle = e^{-(at_1+bt_2)}\frac{e^{(a+b)t_2}}{a+b} = \frac{e^{-a(t_1-t_2)}}{a+b}\Theta(t_1-t_2) \qquad \text{(E.20)}$$

or

$$\langle G_y(t_1,a)G_y(t_2,b)\rangle = e^{-(at_1+bt_2)}\frac{e^{(a+b)t_1}}{a+b} = \frac{e^{-b(t_2-t_1)}}{a+b}\Theta(t_2-t_1)\,. \qquad \text{(E.21)}$$

With the help of (3.25), (E.20), and (E.21),

$$\begin{aligned}
\langle y(t_1)y(t_2)\rangle &= \frac{1}{4(1-s)}\,\langle [G_y(t_1,s_-)-G_y(t_1,s_+)]\,[G_y(t_2,s_-)-G_y(t_2,s_+)]\rangle \\
&= \frac{1}{8s\sqrt{1-s}}\left[s_+e^{-s_-(t_1-t_2)}-s_-e^{-s_+(t_1-t_2)}\right]\Theta(t_1-t_2) \\
&\quad + \frac{1}{8s\sqrt{1-s}}\left[s_+e^{-s_-(t_2-t_1)}-s_-e^{-s_+(t_2-t_1)}\right]\Theta(t_2-t_1)\,. \qquad \text{(E.22)}
\end{aligned}$$

Defining G_Y, which differs from G_y in that $\eta_y(t')$ is replaced by $y(t')$, as

$$G_Y(t,s') \equiv \int_{-\infty}^{t} e^{-s'(t-t')}y(t')\,\mathrm{d}t'\,, \qquad \text{(E.23)}$$

we have

$$\begin{aligned}
\langle G_Y(t,a)G_Y(0,b)\rangle &= \left\langle \int_{-\infty}^{t} e^{-a(t-t_1)}y(t_1)\,\mathrm{d}t_1 \int_{-\infty}^{0} e^{-b(0-t_2)}y(t_2)\,\mathrm{d}t_2 \right\rangle \\
&= \int_{-\infty}^{t}\int_{-\infty}^{0} e^{-a(t-t_1)+bt_2}\,\langle y(t_1)y(t_2)\rangle\,\mathrm{d}t_2\,\mathrm{d}t_1 \\
&= \frac{e^{-at}}{8s\sqrt{1-s}}\left[s_+\int_{-\infty}^{0} e^{(b+s_-)t_2}\int_{t_2}^{t} e^{(a-s_-)t_1}\,\mathrm{d}t_1\,\mathrm{d}t_2\right. \\
&\qquad \left. -s_-\int_{-\infty}^{0} e^{(b+s_+)t_2}\int_{t_2}^{t} e^{(a-s_+)t_1}\,\mathrm{d}t_1\,\mathrm{d}t_2\right] \\
&\quad + \frac{e^{-at}}{8s\sqrt{1-s}}\left[\frac{1}{a+b}\left(\frac{s_+}{a+s_-}-\frac{s_-}{a+s_+}\right)\right]. \qquad \text{(E.24)}
\end{aligned}$$

Copyright © by SIAM. Unauthorized reproduction of this article is prohibited.

Downloaded 10/30/20 to 59.64.129.2. Redistribution subject to SIAM license or copyright; see https://epubs.siam.org/page/terms

More specifically, the cases we really need below are

$$\langle G_Y(t,s_-)G_Y(0,s_-)\rangle = \frac{e^{-s_-t}}{8s\sqrt{1-s}}\left[\frac{s_+t}{2s_-}+\frac{s_+}{4s_-^2}-\frac{s_-}{s_--s_+}\left(\frac{e^{(s_--s_+)t}}{s_-+s_+}-\frac{1}{2s_-}\right)+\frac{b_+}{2s_-}\right],$$

$$\begin{aligned}\langle G_Y(t,s_-)G_Y(0,s_+)\rangle &= \frac{e^{-s_-t}}{8s\sqrt{1-s}}\left[\frac{s_+t}{s_-+s_+}+\frac{s_+}{(s_-+s_+)^2}-\frac{s_-}{s_--s_+}\left(\frac{e^{(s_--s_+)t}}{2s_+}-\frac{1}{s_-+s_+}\right)\right]\\ &\quad+\frac{e^{-s_-t}}{8s\sqrt{1-s}}\left[\frac{1}{s_-+s_+}\left(\frac{s_+}{2s_-}-\frac{s_-}{s_-+s_+}\right)\right],\end{aligned}$$

$$\begin{aligned}\langle G_Y(t,s_+)G_Y(0,s_-)\rangle &= \frac{e^{-s_+t}}{8s\sqrt{1-s}}\left[\frac{s_+}{s_+-s_-}\left(\frac{e^{(s_+-s_-)t}}{2s_-}-\frac{1}{s_-+s_+}\right)-\frac{s_-t}{s_-+s_+}-\frac{s_-}{(s_-+s_+)^2}\right]\\ &\quad+\frac{e^{-s_+t}}{8s\sqrt{1-s}}\left[\frac{1}{s_-+s_+}\left(\frac{s_+}{s_-+s_+}-\frac{s_-}{2s_+}\right)\right],\end{aligned}$$

$$\langle G_Y(t,s_+)G_Y(0,s_+)\rangle = \frac{e^{-s_+t}}{8s\sqrt{1-s}}\left[\frac{s_+}{s_+-s_-}\left(\frac{e^{(s_+-s_-)t}}{s_-+s_+}-\frac{1}{2s_+}\right)-\frac{s_-t}{2s_+}-\frac{s_-}{4s_+^2}+\frac{b_-}{2s_+}\right],$$

where the abbreviation

$$b_\pm = \pm\frac{s_\pm}{2s_\mp}\mp\frac{s_\mp}{s_-+s_+} \tag{E.25}$$

was used. We can rewrite the solution (3.28) as the sum of two uncorrelated parts $x(t)=x_1(t)+x_2(t)$, with

$$x_i(t) = \frac{1}{2\sqrt{1-s}}\left[G_{x_i}(t,s_-)-G_{x_i}(t,s_+)\right], \quad i=1,2, \tag{E.26}$$

and

$$G_{x_1}(t,s') \equiv \int_{-\infty}^{t} e^{-s'(t-t')}2ry(t')\,\mathrm{d}t', \quad G_{x_2}(t,s') \equiv \int_{-\infty}^{t} e^{-s'(t-t')}\eta_x(t')\,\mathrm{d}t'. \tag{E.27}$$

Since $\langle x_2(t)x_2(0)\rangle = \langle y(t)y(0)\rangle$ was calculated above, the remaining contribution to $\langle x(t)x(0)\rangle$ is

$$\begin{aligned}\langle x_1(t)x_1(0)\rangle &= \frac{r^2}{1-s}\left\langle\left[G_Y(t,s_-)-G_Y(t,s_+)\right]\left[G_Y(0,s_-)-G_Y(0,s_+)\right]\right\rangle\\ &= \frac{r^2e^{-s_+t}}{16s(1-s)^{3/2}}\frac{\sqrt{1-s}}{\left(1+\sqrt{1-s}\right)}\left[s_-t+\frac{s_-}{s_+}-\left(\sqrt{1-s}-\frac{1}{\sqrt{1-s}}\right)\right]\\ &\quad+\frac{r^2e^{-s_-t}}{16s(1-s)^{3/2}}\frac{\sqrt{1-s}}{\left(1-\sqrt{1-s}\right)}\left[s_+t+\frac{s_+}{s_-}+\left(\sqrt{1-s}-\frac{1}{\sqrt{1-s}}\right)\right].\end{aligned} \tag{E.28}$$

Multiplying $\left(1-\sqrt{1-s}\right)^2\left(1+\sqrt{1-s}\right)^2 = s^2$ on both sides gives

$$\begin{aligned}s^2\left\langle x_1(t)x_1(0)\right\rangle &= \frac{r^2e^{-s_+t}}{16s(1-s)^{3/2}}\left(1-\sqrt{1-s}\right)^2\left[\sqrt{1-s}\,(st+s+1)+2s-1\right]\\ &\quad+\frac{r^2e^{-s_-t}}{16s(1-s)^{3/2}}\left(1+\sqrt{1-s}\right)^2\left[\sqrt{1-s}\,(st+s+1)-2s+1\right],\end{aligned} \tag{E.29}$$

which brings us into agreement with (3.30d),

$$\langle x(t)x(0)\rangle = \frac{\left(C_1^+ + C_1^-\right)}{8s\sqrt{1-s}} + \frac{r^2\left(B^+ + B^-\right)}{16s^3(1-s)^{3/2}}. \tag{E.30}$$

∎

Copyright © by SIAM. Unauthorized reproduction of this article is prohibited.

Acknowledgments. The authors thank Hans Christian Öttinger, Gabriel Stoltz, and anonymous referees for valuable suggestions and comments.

Downloaded 10/30/20 to 59.64.129.2. Redistribution subject to SIAM license or copyright; see https://epubs.siam.org/page/terms

REFERENCES

[1] A. Abdulle, G. Vilmart, and K. C. Zygalakis, *High order numerical approximation of the invariant measure of ergodic SDEs*, SIAM J. Numer. Anal., 52 (2014), pp. 1600–1622, https://doi.org/10.1137/130935616. (Cited on p. 919)

[2] A. Abdulle, G. Vilmart, and K. C. Zygalakis, *Long time accuracy of Lie–Trotter splitting methods for Langevin dynamics*, SIAM J. Numer. Anal., 53 (2015), pp. 1–16, https://doi.org/10.1137/140962644. (Cited on p. 919)

[3] M. P. Allen and D. J. Tildesley, *Computer Simulation of Liquids*, Oxford University Press, 1989. (Cited on p. 904)

[4] M. Baiesi, E. Boksenbojm, C. Maes, and B. Wynants, *Nonequilibrium linear response for Markov dynamics,* II: *Inertial dynamics*, J. Stat. Phys., 139 (2010), pp. 492–505. (Cited on p. 903)

[5] M. Baiesi, C. Maes, and B. Wynants, *Nonequilibrium linear response for Markov dynamics,* I: *Jump processes and overdamped diffusions*, J. Stat. Phys., 137 (2009), p. 1094. (Cited on p. 903)

[6] O. E. Barndorff-Nielsen, T. Mikosch, and S. I. Resnick, *Lévy Processes: Theory and Applications*, Springer Science & Business Media, 2001. (Cited on p. 904)

[7] R. B. Bird, C. F. Curtiss, R. C. Armstrong, and O. Hassager, *Dynamics of Polymeric Liquids. Volume* 2: *Kinetic Theory*, Wiley-Interscience, 1987. (Cited on p. 903)

[8] H. Block and E. F. Hayes, *Dielectric behavior of stiff polymers in solution when subjected to high voltage gradients*, Trans. Faraday Soc., 66 (1970), p. 2512. (Cited on p. 903)

[9] W. R. Cao, M. Z. Liu, and Z. C. Fan, *MS-stability of the Euler–Maruyama method for stochastic differential delay equations*, Appl. Math. Comput., 159 (2004), pp. 127–135. (Cited on p. 903)

[10] E. A. Codling, M. J. Plank, and S. Benhamou, *Random walk models in biology*, J. Roy. Soc. Interf., 5 (2008), pp. 813–834. (Cited on p. 903)

[11] W. T. Coffey and Y. P. Kalmykov, *The Langevin Equation: With Applications to Stochastic Problems in Physics, Chemistry and Electrical Engineering*, 4th ed., World Scientific, 2017. (Cited on p. 903)

[12] A. Debussche and E. Faou, *Weak backward error analysis for SDEs*, SIAM J. Numer. Anal., 50 (2012), pp. 1735–1752, https://doi.org/10.1137/110831544. (Cited on p. 919)

[13] V. Delgado, J. Breton, A. Hardisson, and C. Girardet, *Generalized Langevin equation approach for the rotational relaxation of a molecule trapped in a* 3*D crystal.* II. *Application to CO and* CH_3F *in argon*, J. Chem. Phys., 87 (1987), pp. 4809–4822. (Cited on p. 903)

[14] M. Doi, *Introduction to Polymer Physics*, Oxford University Press, 1996. (Cited on pp. 903, 904, 907, 922)

[15] M. Doi and S. F. Edwards, *The Theory of Polymer Dynamics*, Oxford University Press, 1988. (Cited on pp. 903, 907)

[16] P. C. Fannin, B. K. P. Scaife, and S. W. Charles, *A study of the complex ac susceptibility of magnetic fluids subjected to a constant polarizing magnetic field*, J. Magn. Magn. Mater., 85 (1990), p. 54. (Cited on p. 903)

[17] R. T. Foister and T. G. M. van de Ven, *Diffusion of Brownian particles in shear flows*, J. Fluid Mech., 96 (1980), pp. 105–132. (Cited on p. 910)

[18] D. Frenkel and B. Smit, *Understanding Molecular Simulation: From Algorithms to Applications*, 2nd ed., Academic Press, 2001. (Cited on p. 904)

[19] C. Gardiner, *Stochastic Methods*, Springer, 2009. (Cited on p. 903)

[20] C. W. Gardiner, *Handbook of Stochastic Methods for Physics, Chemistry and the Natural Sciences*, Springer, 1985. (Cited on p. 917)

[21] M. D. Graham, *Microhydrodynamics, Brownian Motion, and Complex Fluids*, Cambridge University Press, 2018. (Cited on p. 923)

[22] D. J. Higham, *An algorithmic introduction to numerical simulation of stochastic differential equations*, SIAM Rev., 43 (2001), pp. 525–546, https://doi.org/10.1137/S0036144500378302. (Cited on p. 917)

[23] D. J. Higham, X. Mao, and A. M. Stuart, *Strong convergence of Euler-type methods for nonlinear stochastic differential equations*, SIAM J. Numer. Anal., 40 (2002), pp. 1041–1063, https://doi.org/10.1137/S0036142901389530. (Cited on p. 903)

[24] E. J. Hinch, *Application of the Langevin equation to fluid suspensions*, J. Fluid Mech., 72 (1975), pp. 499–511. (Cited on p. 904)

Copyright © by SIAM. Unauthorized reproduction of this article is prohibited.

[25] J. Honerkamp, *Stochastic Dynamical Systems: Concepts, Numerical Methods, Data Analysis*, John Wiley & Sons, 1994. (Cited on pp. 903, 916, 923)
[26] T. Indei, J. D. Schieber, A. Cordoba, and E. Pilyugina, *Treating inertia in passive microbead rheology*, Phys. Rev. E, 85 (2012), art. 021504. (Cited on p. 904)
[27] K. Isoda, N. Kouchi, and Y. Hatano, *The effect of an external electric field on diffusion-controlled bulk ion recombination*, J. Chem. Phys., 100 (1994), pp. 5874–5881. (Cited on p. 903)
[28] P. E. Kloeden and E. Platen, *Numerical Solution of Stochastic Differential Equations*, Springer, 1992. (Cited on p. 917)
[29] K. Kremer and G. S. Grest, *Dynamics of entangled linear polymer melts: A molecular-dynamics simulation*, J. Chem. Phys., 92 (1990), pp. 5057–5086. (Cited on pp. 904, 908)
[30] M. Kröger, *Models for Polymeric and Anisotropic Liquids*, Springer Science & Business Media, 2005. (Cited on p. 923)
[31] M. Kröger and M. Hütter, *Unifying kinetic approach to phoretic forces and torques onto moving and rotating convex particles*, J. Chem. Phys., 125 (2006), art. 044105. (Cited on p. 903)
[32] M. Kröger, W. Loose, and S. Hess, *Rheology and structural changes of polymer melts via nonequilibrium molecular dynamics*, J. Rheol., 37 (1993), pp. 1057–1079. (Cited on pp. 904, 908)
[33] J. P. Larentzos, J. K. Brennan, J. D. Moore, M. Lísal, and W. D. Mattson, *Parallel implementation of isothermal and isoenergetic dissipative particle dynamics using Shardlow-like splitting algorithms*, Comput. Phys. Commun., 185 (2014), pp. 1987–1998. (Cited on p. 918)
[34] B. Leimkuhler and C. Matthews, *Rational construction of stochastic numerical methods for molecular sampling*, Appl. Math. Res. Express, 2013 (2013), pp. 34–56. (Cited on pp. 918, 919)
[35] B. Leimkuhler and C. Matthews, *Robust and efficient configurational molecular sampling via Langevin dynamics*, J. Chem. Phys., 138 (2013), art. 174102. (Cited on pp. 919, 921)
[36] B. Leimkuhler and C. Matthews, *Molecular Dynamics: With Deterministic and Stochastic Numerical Methods*, Springer, 2015. (Cited on pp. 904, 917, 919)
[37] B. Leimkuhler, C. Matthews, and G. Stoltz, *The computation of averages from equilibrium and nonequilibrium Langevin molecular dynamics*, IMA J. Numer. Anal., 36 (2016), pp. 13–79. (Cited on p. 919)
[38] B. Leimkuhler, C. Matthews, and M. V. Tretyakov, *On the long-time integration of stochastic gradient systems*, Proc. R. Soc. Lond. Ser. A Math. Phys. Eng. Sci., 470 (2014), art. 20140120. (Cited on pp. 918, 919)
[39] B. Leimkuhler and X. Shang, *On the numerical treatment of dissipative particle dynamics and related systems*, J. Comput. Phys., 280 (2015), pp. 72–95. (Cited on pp. 919, 920)
[40] B. Leimkuhler and X. Shang, *Adaptive thermostats for noisy gradient systems*, SIAM J. Sci. Comput., 38 (2016), pp. A712–A736, https://doi.org/10.1137/15M102318X. (Cited on p. 919)
[41] B. Leimkuhler and X. Shang, *Pairwise adaptive thermostats for improved accuracy and stability in dissipative particle dynamics*, J. Comput. Phys., 324 (2016), pp. 174–193. (Cited on pp. 919, 920)
[42] M. Lísal, J. K. Brennan, and J. B. Avalos, *Dissipative particle dynamics at isothermal, isobaric, isoenergetic, and isoenthalpic conditions using Shardlow-like splitting algorithms*, J. Chem. Phys., 135 (2011), art. 204105. (Cited on p. 918)
[43] S. Litvinov, M. Ellero, X. Hu, and N. Adams, *A splitting scheme for highly dissipative smoothed particle dynamics*, J. Comput. Phys., 229 (2010), pp. 5457–5464. (Cited on p. 918)
[44] I. Loncaric, M. Alducin, P. Saalfrank, and J. L. Juaristi, *Femtosecond-laser-driven molecular dynamics on surfaces: Photodesorption of molecular oxygen from Ag*(110), Phys. Rev. B, 93 (2016), art. 014301. (Cited on p. 903)
[45] J. R. Manning, *Diffusion in a chemical concentration gradient*, Phys. Rev., 124 (1961), pp. 470–482. (Cited on p. 903)
[46] M. Manosas, J.-D. Wen, P. T. X. Li, S. B. Smith, C. Boustamante, I. Tinoco, and F. Ritort, *Force unfolding kinetics of RNA using optical tweezers:* II. *Modeling experiments*, Biophys. J., 92 (2007), pp. 3010–3021. (Cited on p. 903)
[47] S. Melchionna, *Design of quasisymplectic propagators for Langevin dynamics*, J. Chem. Phys., 127 (2007), art. 044108. (Cited on p. 918)
[48] G. N. Milstein and M. V. Tretyakov, *Stochastic Numerics for Mathematical Physics*, Springer, 2004. (Cited on p. 917)

Downloaded 10/30/20 to 59.64.129.2. Redistribution subject to SIAM license or copyright; see https://epubs.siam.org/page/terms

Copyright © by SIAM. Unauthorized reproduction of this article is prohibited.

[49] H. Mizuno and R. Yamamoto, *Mechanical responses and stress fluctuations of a supercooled liquid in a sheared non-equilibrium state*, Eur. Phys. J. E, 35 (2012), art. 9707. (Cited on p. 903)
[50] C. R. Nelson and C. R. Plosser, *Trends and random walks in macroeconomic time series: Some evidence and implications*, J. Monet. Econ., 10 (1982), pp. 139–162. (Cited on p. 903)
[51] B. Øksendal, *Stochastic Differential Equations: An Introduction with Applications*, Springer, 2003. (Cited on p. 908)
[52] H. Orihara and Y. Takikawa, *Brownian motion in shear flow: Direct observation of anomalous diffusion*, Phys. Rev. E, 84 (2011), art. 061120. (Cited on p. 908)
[53] H. C. Öttinger, *Stochastic Processes in Polymeric Fluids: Tools and Examples for Developing Simulation Algorithms*, Springer Science & Business Media, 1996. (Cited on p. 903)
[54] J. Ramírez, S. K. Sukumaran, B. Vorselaars, and A. E. Likhtman, *Efficient on the fly calculation of time correlation functions in computer simulations*, J. Chem. Phys., 133 (2010), art. 154103. (Cited on p. 923)
[55] A. Rodkina and H. Schurz, *Almost sure asymptotic stability of drift-implicit θ-methods for bilinear ordinary stochastic differential equations in* $\mathbb{R}^1$, J. Comput. Appl. Math., 180 (2005), pp. 13–31. (Cited on p. 903)
[56] P. E. Rouse, *A theory of the linear viscoelastic properties of dilute solutions of coiling polymers*, J. Chem. Phys., 21 (1953), pp. 1272–1280. (Cited on pp. 903, 922)
[57] J. D. Schieber and H. C. Öttinger, *The effects of bead inertia on the Rouse model*, J. Chem. Phys., 89 (1988), pp. 6972–6981. (Cited on p. 903)
[58] X. Shang, M. Kröger, and B. Leimkuhler, *Assessing numerical methods for molecular and particle simulation*, Soft Matter, 13 (2017), pp. 8565–8578. (Cited on p. 919)
[59] T. Shardlow, *Splitting for dissipative particle dynamics*, SIAM J. Sci. Comput., 24 (2003), pp. 1267–1282, https://doi.org/10.1137/S1064827501392879. (Cited on p. 918)
[60] D. Talay and L. Tubaro, *Expansion of the global error for numerical schemes solving stochastic differential equations*, Stoch. Anal. Appl., 8 (1990), pp. 483–509. (Cited on p. 919)
[61] C. Van den Broeck, J. M. Sancho, and M. San Miguel, *Harmonically bound Brownian motion in flowing fluids*, Phys. A, 116 (1982), pp. 448–461. (Cited on p. 908)
[62] N. G. van Kampen, *Stochastic Processes in Physics and Chemistry*, 3rd ed., Elsevier, 2007. (Cited on p. 903)
[63] D. C. Venerus and H. C. Öttinger, *A Modern Course in Transport Phenomena*, Cambridge University Press, 2018. (Cited on p. 904)
[64] G. Vilmart, *Postprocessed integrators for the high order integration of ergodic SDEs*, SIAM J. Sci. Comput., 37 (2015), pp. A201–A220, https://doi.org/10.1137/140974328. (Cited on p. 918)
[65] M. C. Wang and G. E. Uhlenbeck, *On the theory of the Brownian motion* II, Rev. Mod. Phys., 17 (1945), pp. 323–342. (Cited on p. 913)
[66] N. Willenbacher, C. Oelschlaeger, M. Schopferer, P. Fischer, F. Cardinaux, and F. Scheffold, *Broad bandwidth optical and mechanical rheometry of wormlike micelle solutions*, Phys. Rev. Lett., 99 (2007), art. 068302. (Cited on p. 904)
[67] X. Yang and C. C. Church, *A simple viscoelastic model for soft tissues the frequency range 6-20 MHz*, IEEE Trans. Ultrason. Ferroelectr. Freq. Control, 53 (2006), pp. 1404–1411. (Cited on p. 903)

Downloaded 10/30/20 to 59.64.129.2. Redistribution subject to SIAM license or copyright; see https://epubs.siam.org/page/terms

Copyright © by SIAM. Unauthorized reproduction of this article is prohibited.